HUNGARIAN UNIVERSITY OF AGRICULTURE AND LIFE SCIENCES

THESIS OF DOCTORAL (PhD) DISSERTATION

MOSTAFA AHMED ABDALMAGEED

Keszthely

2026

HUNGARIAN UNIVERSITY OF AGRICULTURE AND LIFE SCIENCES

Insights on Physiological and Transcriptomic Evaluation of Zinc Oxide Nanoparticle-Mediated Salinity Stress Tolerance in *Solanum lycopersicum* L. and *Zea mays* L.

By:

MOSTAFA AHMED ABDALMAGEED

Georgikon Campus

Keszthely

2026

The Doctoral School

Name: DOCTORAL SCHOOL OF NATURAL SCIENCES

Discipline: ENVIRONMENTAL SCIENCES

Specialization: AGRICULTURAL SCIENCES (AGRICULTURAL BIOCHEMISTRY)

Head:

Dr. ERIKA CSÁKINÉ MICHÉLI
University Professor, Institute Director, Head of Department, Szent István Campus, Gödöllő
Full member of the Hungarian Academy of Sciences
Doctoral School of Natural Sciences

Supervisors:

Dr. ZOLTÁN TÓTH
Associate Professor, PhD
Institute of Agronomy, Doctoral School of Food and Agriculture Sciences, Georgikon Campus, Keszthely

Dr. KINCSŐ DECSI
Associate Professor, PhD
Institute of Agronomy, Doctoral School of Food and Agriculture Sciences, Georgikon Campus, Keszthely

....
Approval of the Head of Doctoral School Approval of the Supervisor (1)

.....
Approval of the Supervisor (2)

Table of Contents

1. SHORT INTRODUCTION AND OBJECTIVES

Crop plants' physiological and biochemical pathways are adversely affected by soil salinity through a complex mechanism (Nabati et al., 2011). When there is too much Na^+ in the cell, cytosolic K^+ and Ca^{2+} leave the cell. This upsets the balance of their homeostasis, which leads to nutritional deficiencies, oxidative stress, slowed growth, and cell death (Ahanger et al., 2015). Several stomatal restrictions, such as stomatal closure (Munns and Tester, 2008) and non-stomatal limitations like chlorophyll dysfunction (Jiang et al., 2017), deprivation of enzymatic proteins and membranes of the photosynthetic apparatus (Mittal et al., 2012), and chloroplast ultrastructure destruction (Gengmao et al., 2015), have been reported to have a significant negative impact on plant photosynthesis at high salinization levels, salt-affected soils demonstrate higher Na^+/K^+ and Na^+/Ca^{2+} ratios due to the increased presence of Na^+ in the soil solution. Consequently, a reduction in the uptake of potassium ions (K^+) and calcium ions (Ca^{2+}) might hinder cellular functioning, resulting in the destabilization of cell membranes and the impairment of enzymatic activity, which is facilitated by the enzymes (Quintero et al., 2007). The production of too many reactive oxygen substances/species (ROS) in the cytosol, chloroplast, and mitochondria is influenced by osmotic pressure and ionic toxicity, leading to oxidative damage (Abbasi et al., 2015; Munns and Tester, 2008). These reactive oxygen species can damage plant tissues, alter the double-helical DNA, disrupt the phospholipid bilayer (Noctor and Foyer, 1998), degrade the active biomolecules like lipids and proteins, and destroy photoreceptors like phytochromes A and B (Pitzschke et al., 2006).

On a global scale, there is significant consumption of both fresh and processed tomatoes (*Solanum lycopersicum* L.). Therefore, a widely consumed functional food can be ingested by individuals worldwide, either in its uncooked or cooked state, or as a primary ingredient that undergoes processing to create various products such as tomato powder, juice, puree, sauces, ketchup, and paste (Chabi et al., 2024; Li et al., 2021).

Every year, a multitude of factors can impact the nutritional quality and quantity of tomatoes (Inculet et al., 2019). Agricultural crop productivity and cultivation are impacted by a variety of environmental difficulties, including strong winds, extreme temperatures, soil salinity, drought, and flooding (Shrivastava and Kumar, 2015).

Maize, scientifically known as *Zea mays* L., is a versatile crop that can thrive in various agro-climatic conditions. It is cultivated in various regions worldwide, reaching elevations up to 3000 m above sea level (Sah et al., 2020). Farmers like this crop because it has the largest grain production potential among cereals (Pandit et al., 2016; Sah et al., 2020). It can be used for both grain and fodder (Chaudhary et al., 2016; Sah et al., 2016), and is also

grown as a cash crop for specialized corn varieties such as green ear, baby corn, sweet corn, and popcorn (Manigopa and Sah, 2012).

It has been observed that zinc oxide nanoparticles (ZnO-NPs) have important and essential functions in promoting plant growth and enhancing plant resistance to salt stress in several plant species (Gaafar et al., 2020). Zinc (Zn^{2+}) is a crucial micronutrient that is necessary for the proper functioning of living organisms' metabolism (Natasha et al., 2022). It carries out vital duties by participating in the activities of many enzymes (Cuajungco et al., 2021) and serves as a regulatory cofactor in protein synthesis. Moreover, a lack of Zn^{2+} results in the decrease of multiple metabolic processes, including growth, ultimately affecting crop yields (Khan et al., 2022).

A revolution in biology has been brought about by next-generation sequencing, sometimes known as NGS. The production of libraries is necessary for next-generation sequencing (NGS), which involves fusing DNA or RNA molecules as fragments with adapters. A technology known as high-throughput complementary DNA sequencing (RNA-Seq) is an efficient method for analyzing the entire transcriptome (Parkhomchuk et al., 2009). This approach indicates the level of transcript expression, the quality of synthesis, and comprehends how the functionality of differentially expressed genes is crucial for elucidating complex biological processes.

This dissertation explored how chemically synthesized ZnO-NPs alleviate salt stress in *Solanum lycopersicum* L. and *Zea mays* L. This study used dual-protection to investigate ZnO-NPs' effects on biological organization, from field and greenhouse-scale agronomic studies to *in silico* molecular docking. ZnO-NPs may have increased abiotic salt tolerance and initiated biotic plant defense in complex agricultural settings.

Plant-morphological, physiological, biochemical, and transcriptome adaptations for 150 mM NaCl survival were examined. To prove the crop's bioactivity, the scientists purposely combined antibacterial and molecular docking studies. In field and greenhouse environments, ZnO-NPs increased plant vitality and secondary metabolite chemical efficacy to assess cross-tolerance.

Our analysis was based on transcriptome data demonstrating significant proline and thiamine production control. These genetic changes were confirmed and functional by antimicrobial testing and molecular docking. These studies examined bioactive ligands like rutin's biological efficacy against infections in addition to computational obstacles. This comprehensive approach showed that tolerance must be tested by conserving biomass and enhancing nutritional and therapeutic properties, turning salt-stressed leaves into potent antibacterial extracts.

2. MATERIALS AND METHODS

2.1. Design, preparations, and equipment for tomato planting

The experiment involved tomato seeds of the variety Kecskemétii 549 *Solanum lycopersicum* L., which were sterilized with 70% ethanol and washed three times. After one month, the seeds were transplanted into pots and placed in a greenhouse with varying humidity and temperature. Six treatments were applied, including; T1: control treatment (irrigation with distilled water "dw"), T2: irrigation with distilled water + foliar spray of ZnO-NPs (75 mg/L), T3: irrigation distilled water + foliar spray of ZnO-NPs (150 mg/L), T4: irrigation with saline solutions (150 mM NaCl), T5: irrigation with saline solutions (150 mM NaCl) + foliar spray of ZnO-NPs (75 mg/L), and T6: irrigation with saline solutions (150 mM NaCl) + foliar spray of ZnO-NPs (150 mg/L).

The NaCl stress solution was applied to provide salt stress, while a foliar spray of ZnO-NPs was applied three times at different times to include vegetative and generative phases. The moisture content and water-holding capacity of the soil peat mixture were determined by the gravimetric method (Imakumbili et al., 2021) to quantify the amount of irrigation to be supplied to control and treated pots.

2.2. Layout, scheduling, and implementation for growing maize plants

The study used FAO P0023 *Zea mays* L. maize on sandy loam soil with physicochemical properties such as water percentage, bulk density, pH, organic matter content, and electric conductivity. The soil was irrigated every 10 days, with treatments including (1) control treatment, irrigation only with tap water, (2) irrigation with saline solution (150 mM sodium chloride solution), (3) irrigation with 150 mM sodium chloride solution + 2 g/L ZnO-NPs, and (4) irrigation with tap water +2 g/L ZnO-NPs.

Foliar ZnO-NPs were applied using a handheld aerosol-propelled sprayer. The cumulative amount of water given from the start of planting treatments till the harvest was determined using the FAO CROPWAT 0.8 and CLIMWAT 0.2 software. Plants were harvested 142 days after sowing and post-harvest measurements were applied using two different plants from each replicate.

2.3. Chemical synthesis of zinc oxide nanoparticles

ZnO nanoparticles were synthesized by the precipitation method using zinc nitrate hexahydrate "$Zn(NO_3)_2{\cdot}6H_2O$, thermos scientific A16282, LOT: 10242486" and sodium hydroxide "NaOH, 98.5–100.5%, pellets, AnalaR NORMAPUR® Reag. Ph. Eur. analytical reagent" as precursors. ZnO nanoparticles were produced by mixing aqueous solutions of zinc nitrate and sodium hydrate. ZnO nanoparticles were formed by the reaction between Zn^{2+} and hydroxide ions as shown by the following equations (Nejati et al., 2011);

(1) $Zn(NO_3)_2 \rightarrow Zn^{2+} + 2NO^{3-}$ (2) $Zn^{2+} + 2OH^{-} \rightarrow Zn(OH)_2$ (3) $Zn(OH)_2 \rightarrow ZnO + H_2O$.

2.4. Characterization of chemically synthesized zinc oxide nanoparticles

The optical properties of ZnO-NPs were studied using UV-VIS absorption spectroscopy (Zak et al., 2011c). XRD measurements were conducted at Cairo University's Micro Analytical Center (Zak et al., 2011c). FTIR spectra were recorded using a Bruker Vertex 70v with a Bruker Diamond ATR compartment at Nanolab, Pannon University, Hungary (Zak et al., 2011c). The Micro Analytical Center at Cairo University conducted transmission electron microscope investigations using a FEI Talos F200X type microscope. Sample composition was analyzed using an EDAX spectrometer. Both scanning and conventional TEM images were recorded, using MilliQ samples prepared from aqueous dispersion (Solaiman et al., 2020). Dynamic light scattering (DLS) was used to measure the hydrodynamic size and zeta potential of ZnO-NPs. The Zetasizer Nano-ZS uses laser Doppler velocimetry (LDV) to measure the Zeta potential of particles in a solution (Murdock et al., 2008).

2.5. Determination of proline and protein contents

Fresh 500 mg leaf samples were extracted with sulfosalicylic acid. The extraction also used equal amounts of glacial acetic acid and acidic ninhydrin. After heating at 100 °C, 4 mL of toluene was added to the samples. A Genesys (PG Instruments Ltd., T 80, Lutterworth, UK) spectrophotometer evaluated the aspirated layer's absorbance at 520 nm. Proline concentration was measured in micrograms per gram FW (Bates et al., 1973). To determine the protein content, a homogenized 1 g of newly generated leaves was added into a protein extraction buffer. The buffer contained 10 mM tris-HCl (pH = 8.1), 5 mM β-mercaptoethanol, 0.57 mM PMSF, and 10 mM pH 8 EDTA. The mixture was then centrifuged for 10 min at 17,709× g. After gathering the liquid, Bradford reagent was used to induce the color. A Genesys (PG Instruments Ltd., T 80, UK) spectrophotometer measured the color intensity at 595 nm, and the protein concentration was presented in micrograms per gram FW (Bradford, 1976).

2.6. Determination of total free amino acids

The fresh leaves were pulverized into a fine powder using a mortar and pestle. The resulting powder was then mixed with 10 mL of phosphate buffer solution, which had a concentration of 0.05 M. The pulverized leaves were centrifuged at 12,298× g for 10 min at 4 °C. The reaction mixture in a test tube contained 0.5 mL of the extract, 0.5 mL of 4% ninhydrin, and 0.5 mL of 2% pyridine. The test tubes were vigorously vortexed and heated at 100 °C for 30 min in a water bath. The optical density at 570 nm was measured using a

spectrophotometer (Genesys PG Instruments Ltd., T 80, UK) (Zafar et al., 2022).

2.7. Determination of total hydrolyzable sugars

The total soluble sugars were extracted and estimated using a significantly modified method. Dry tissue was immersed in 5 mL of 2.5 N HCl in a boiling water bath for 3 h with agitation to extract soluble sugars. Finally, the samples were centrifuged at 3075× *g*. The extracts were boiled for 10 min with 3.0 mL of freshly prepared anthrone and chilled to quantify total soluble sugars. The spectrophotometer (Genesys PG Instruments Ltd., T 80, UK) measured the green color intensity at 630 nm absorbance (Prud'homme et al., 1992).

2.8. Determination of lipid peroxidation

A slightly modified method used malondialdehyde (MDA) concentration to quantify lipid peroxidation. During this process, 100 mg of fresh plant leaves were well mixed in 1 mL of 0.1% TCA. After vigorous mixing, the tubes were centrifuged at 20,784× *g* at 4 °C for 10 min. In a Falcon tube, 800 microliters of centrifuged liquid were mixed with 2 milliliters of 0.5% TBA solution. A water bath heated the mixture to 80 °C for 25 min. After incubation, the tubes were chilled on ice for 5 min and centrifuged at 20,784× *g* at 4 °C for 10 min to separate and collect any remaining TBA. Using a Genesys (PG Instruments Ltd., T 80, UK) spectrophotometer at 532 and 600 nm, optical density was determined (Heath and Packer, 1968).

2.9. Determination of hydrogen peroxide (H_2O_2)

The fresh leaves, weighing approximately 0.5 g, were crushed in 5 mL of a solution containing 0.1% (*w*/*w*) trichloroacetic acid. The resulting mixture was centrifuged at 17,709× *g* for 15 min. Phosphate buffer with a pH of 7.2 and a concentration of 100 mM, and potassium iodide were added into a 0.5 mL solution of the reaction mixture. The achieved color was measured using a UV-visible spectrophotometer (Genesys PG Instruments Ltd., T 80, UK), which measured the absorbance of the mixture at a wavelength of 390 nm (Alexieva et al., 2001).

2.10. Determination of total flavonoid compounds (TFCs)

The flavonoid levels in tomato aqueous extracts were assessed using the aluminum chloride colorimetric technique. Test tubes filled with tomato leaf extract were mixed with 5% sodium nitrite, 10% aluminum chloride, and 1 M sodium hydroxide. The tubes were incubated for 15 min, and the absorbance of the pink color was measured using a spectrophotometer (Genesys PG Instruments Ltd., T 80, UK) at 510 nm. Quercetin was used as a standard substance, and the total flavonoid content was quantified as the amount of Quercetin equivalent in micrograms per gram of dry extract (Ahmed et al., 2023b).

2.11. Determination of total phenolic compounds (TPCs)

The phenolic content of tomato leaves was quantified using the Folin–Ciocalteu reagent method. The extract was adjusted to 2500 µg/mL and added to a solution of 1 N Folin–Ciocalteu reagent and 20% sodium carbonate. The mixture was kept in a dark environment for 90 min. The blue color was measured at 650 nm using a spectrophotometer (Genesys PG Instruments Ltd., T 80, UK), and the total phenolic content was determined by calculating the equivalent amount of Gallic acid in micrograms per gram of dry extract (Ahmed et al., 2023b).

2.12. Estimation of enzyme activities

Table 1. A summary of the protocols used to determine the activities of the antioxidative enzymes.

Process	Components	Measurement	Reference
Enzymatic Extracting Buffer	50 mM sodium phosphate buffer (pH 7.5) M PMSF stock: 0.17 g PMSF 8 % (*w/v*) polyvinylpyrolydone (PVP) (Av. Mwt: 10000) 0.01 % (*v/v*) Triton X-100		(Venisse et al., 2001)
Estimation of Peroxidase	100 mM phosphate buffer (pH 6) Pyrogallol Solution 5% [*w/v*] Hydrogen Peroxide H_2O_2 (0.50%) [*v/v*]	The absorbance was measured at 420 nm	(Chance and Maehly, 1955)
Estimation of Glutathione Reductase	0.2 M Tris/HCl buffer (pH 7.8) 3 mM EDTA (Mwt: 292.24) 0.2 mM NADPH (Mwt: 833) 0.5 mM oxidized glutathione (M.wt: 612.7)	The absorbance was measured at 340 nm	(Venisse et al., 2001)
Estimation of Glutathione-S-Transferase	0.1 M potassium phosphate (pH 6.5) 3.6 mM reduced glutathione (Mwt: 307.3) 1 mM 1-chloro-2,4-dinitrobenzene (Mwt: 202.55)	The absorbance was measured at 340 nm	(Habig et al., 1974)
Estimation of Superoxide dismutase	50 mM phosphate buffer (pH = 7.8) 20 µM riboflavin (Mwt: 376.36) 75 mM nitroblue tetrazolium chloride (Mwt: 817.64) 13 mM methionine (Mwt: 149.21)	The absorbed bluish color was observed and measured at 560 nm	(Beauchamp and Fridovich, 1971)

	0.1 mM ethylene diamine tetra acetic acid (EDTA) (Mwt: 292.24)		
Estimation of Catalase	0.1 M H_2O_2 solution 10% H_2SO_4 solution 0.05 N $KMnO_4$ (Eq.wt: 31.6) solution	Catalase activity was expressed in terms of mg H_2O_2 decomposed/gram of fresh weight of tissue/1 mL of 0.05 N $KMnO_4$ = 17 mg of H_2O_2.	(Bonnichsen et al., 1947; Maehly, 1954)

2.13. Transcriptomic analysis

Leaf tissue samples were collected from each plant in experimental treatments and stored at -20°C until further procedures were performed. Messenger RNA (mRNA) was obtained using paramagnetic NEXTFLEX® Poly(A) Beads 2.0 and the NEXTFLEX® Rapid Directional RNA-Sequence Kit 2.0. Illumina NovaSeq 6000 technology was used for genome sequencing, using a deep sequencing technique. FastQC software was used to evaluate and adjust quality parameters. Secondary pre-filtration of raw readings was performed using the Trimmomatic tool. The cleaned, filtered SRA datasets from treatments were used to construct the *de novo* transcriptome, aiming to generate longer contigs from intermediate reads and improve interpretability. Quantifying the transcript level was used to determine the extent of transcripts' biological expression. A count table was generated to examine genes and determine individual expression levels. When numerous treatments were administered, transcript expression levels within each treatment were evaluated, allowing for accurate measurement of differences in gene expression levels among treatments.

The study analyzed the differential expression of genes in tomato and maize plants. The analysis was performed in seven combinations for the tomato experiment, including non-treated and salinity-stressed plants, sprayed plants with different concentrations of ZnO-NPs, and sprayed plants with different concentrations of ZnO-NPs. The comparisons for tomatoes were summarized as follows: 1- T1 vs T4, 2- T1 vs T2, 3- T1 vs T5, 5- T1 vs T6, 6- T4 vs T5, 7- T4 vs T6. For the maize experiment, the analysis was performed in four combinations as follows: 1- M1 vs M2. 2- M1 vs M3. 3- M1 vs M4. 4- M2 vs M3.

In the next step, functional analysis was applied to the dataset to identify transcriptomic contigs obtained from the step of *de novo* assembly. The unidentified contigs were transformed into a defined, mapped, and annotated dataset, with each contig accompanied by relevant metadata. The results showed what the biological role of the sequence was and how it was involved in a number of metabolic processes. This work utilized OmicsBox

Biobam software to generate an annotation table through the analysis of Gene Ontology (GO) https://www.biobam.com/omicsbox/ (accessed May 14, 2025) (OmicsBox, 2019).

2.14. Determination of the antimicrobial activity

Table 2. Experimental parameters for antimicrobial susceptibility testing and media composition.

Category	Details and specific components
Bacterial strains	Gram-positive: *Staphylococcus aureus* ATCC 13565 and *Bacillus cereus* EMCC 1080 Gram-negative: *Listeria monocytogenes* LMD 7726, *Pseudomonas aeruginosa* NRRL B-272, *Escherichia coli* O157:H7 ATCC 51659, and *Salmonella typhi* ATCC 25566
Fungal isolates	*Aspergillus niger* SSWT 2999, *Aspergillus ochraceus* ITAL 14, *Aspergillus flavus NRRL 3357*, *Fusarium proliferatum* MPVP 328, *Fusarium verticilloides* ITEM 10027, *and Penicillium verrucosum* BFE 500
Growth media	**Nutritional Agar:** Meat extract (1g), Yeast extract (2g), Peptone (5g), NaCl (5g), Agar (15g); pH 7.4±0.2 (A.T.C.C., 1984; Tsubouchi et al., 1987) **TSB:** Casein/Soybean digests, Dextrose, NaCl, K_2HPO_4; pH 7.3±0.2 **PDA:** [Potato (200g), Glucose (15g), Agar (20 g)] L^{-1}
Standardization	**0.5 McFarland Standard:** $BaSO_4$ solution ($BaCl_2.2H_2O$ + H_2SO_4); Absorbance 0.08–0.1 at 625 nm (10^8 cfu mL^{-1})
Disc diffusion (bacteria)	**Method:** Kirby-Bauer (Bauer et al., 1996) **Concentration**: 5 mg mL^{-1} in DMSO; Disc: 6 mm **Temp/Time:** 37°C for 24 hours **Controls:** DMSO (−Ve) / Tetracycline 0.5 mg mL^{-1} (+Ve)
Disc diffusion (fungi)	**Method:** Yeast extract supplementary (YES) medium with 0.01% Tween 80 (Medeiros et al., 2011) **Temp/Time:** 25°C for 48 hours **Controls:** DMSO (−Ve) / Nystatin 1000 U mL^{-1} (+Ve) Negative control results showed no inhibition in any bacterial/fungal strains.
MIC determination	**Bacteria:** Tube dilution in TSB; 37°C for 24 hours (Wiegand et al., 2008) **Fungi:** PDA incorporation method (extract + molten PDA + Tween 80); 25°C for 48 hours (Maurya et al., 2019)

2.15. The docking of molecules characterization

A molecular docking study was conducted using the Molecular Operating Environment software (version 2014.09) to evaluate the antibacterial activity of tomato and maize leaf extracts and corroborate the *in vitro* findings. For tomato, the Topoisomerase II ATPase enzyme (DNA Gyrase) (PDB Id: 3TTZ) served as an antibacterial target, while the sterol 14-alpha demethylase (CYP51) protein (PDB Id: 5FSA) was utilized as an antifungal target. For maize, the Topoisomerase II ATPase enzyme (DNA Gyrase) (PDB Id: 6F86) served as an antibacterial target, and the alpha-L-fucosidase (PDB Id: 9LXL) was utilized as as an antifungal target. The 17 compounds discovered by HPLC in our current study -for both plants- were evaluated within the active site of both targets. Two-dimensional structures of all tested compounds were generated using MOE using SMILES codes received from the National Library of Medicine (https://pubchem.ncbi.nlm.nih.gov/).

2.16. Statistical analysis

The experimental techniques in this study consisted of performing all assessments four times, and the resulting values were reported as the average, together with the standard error. The statistical analysis was performed utilizing the Web Agri Stat Package (WASP) (Ahmed et al., 2023c) and JASP (Berkhout et al., 2024; Hoffmann et al., 2022) software. The study used a one-way analysis of variance (ANOVA) to investigate differences between groups. The Tukey test was employed using significance thresholds of 5%.

3. RESULTS

3.1. Characterization of chemically synthesized ZnO-NPs

Figure 1 displayed the spectrum of a distinct absorption peak of ZnO at a wavelength of 370 nm, which corresponds to the intrinsic band-gap absorption of ZnO. This absorption is caused by electron transitions from the valence band to the conduction band ($O_{2p} \rightarrow Zn_{3d}$).

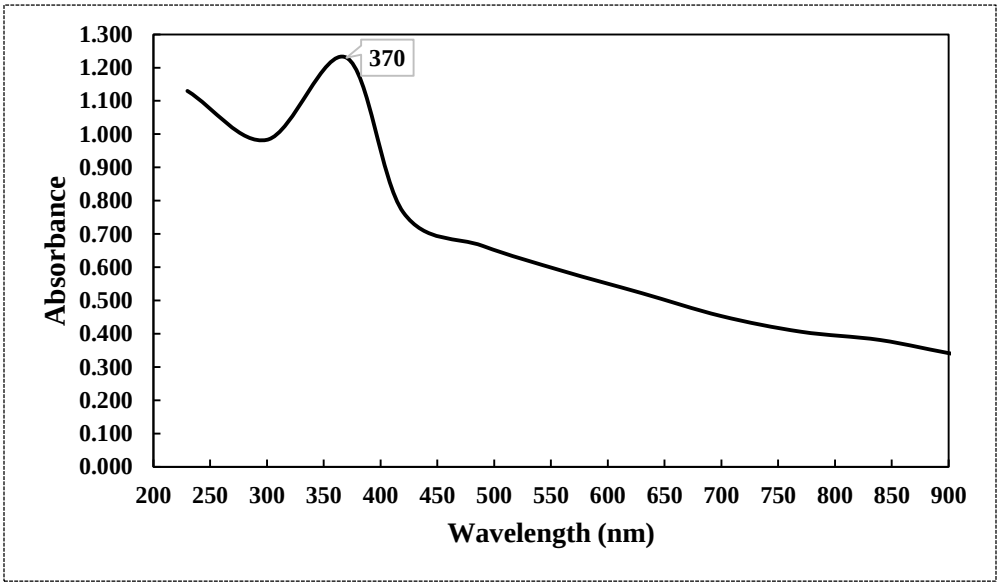

Figure 1. UV.VIS spectrum of chemically synthesized ZnO-NPs.

Figures 2–4 and Table 1 displayed the transmission electron microscopy (TEM), scanning electron microscopy (SEM), energy-dispersive X-ray spectroscopy (EDAX), and size distribution of the zinc oxide nanoparticles (ZnO-NPs) that were synthesized using the precipitation method. The transmission electron microscopy (TEM) image (Figure 2) revealed that the ZnO nanoparticles (NPs) have developed in a nearly hexagonal morphology, indicating the high quality of the ZnO-NPs. Figure 3 displayed the scanning electron microscope (SEM) images of the ZnO-NPs, revealing a uniform shape and size for the particles. Furthermore, the presence of ZnO-NPs in the powder form is evident. Figure 4 confirmed that the primary constituents of the ZnO sample consist of zinc (Zn) and oxygen (O), which were evenly distributed across the surface of the ZnO nanoparticles. The size distribution of the ZnO-NPs produced using the precipitation method at a calcination temperature of 200 °C for 2 h was monomodal with a half-width of approximately 41.166 nm.

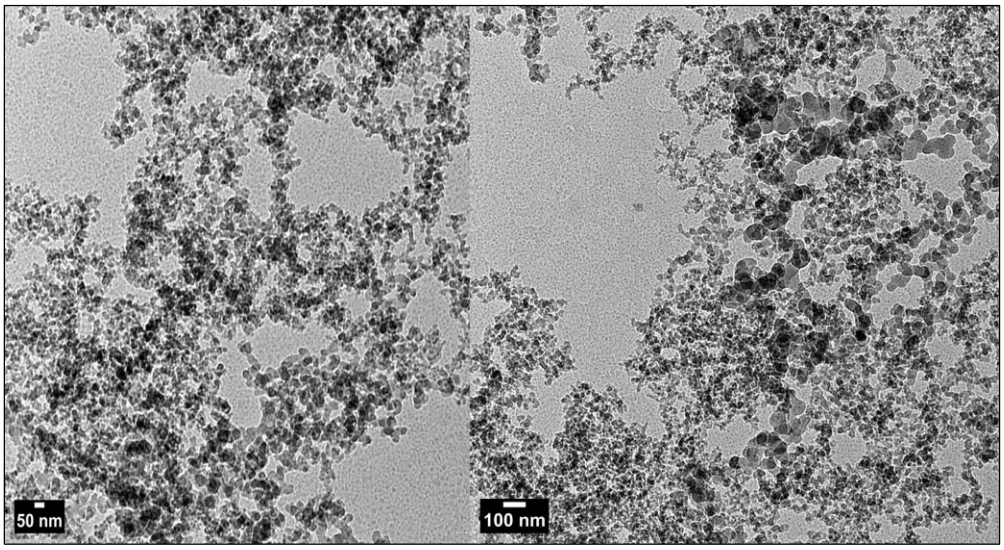

Figure 2. Electron micrographs (TEM) of chemically synthesized ZnO-NPs on 50 and 100 nm.

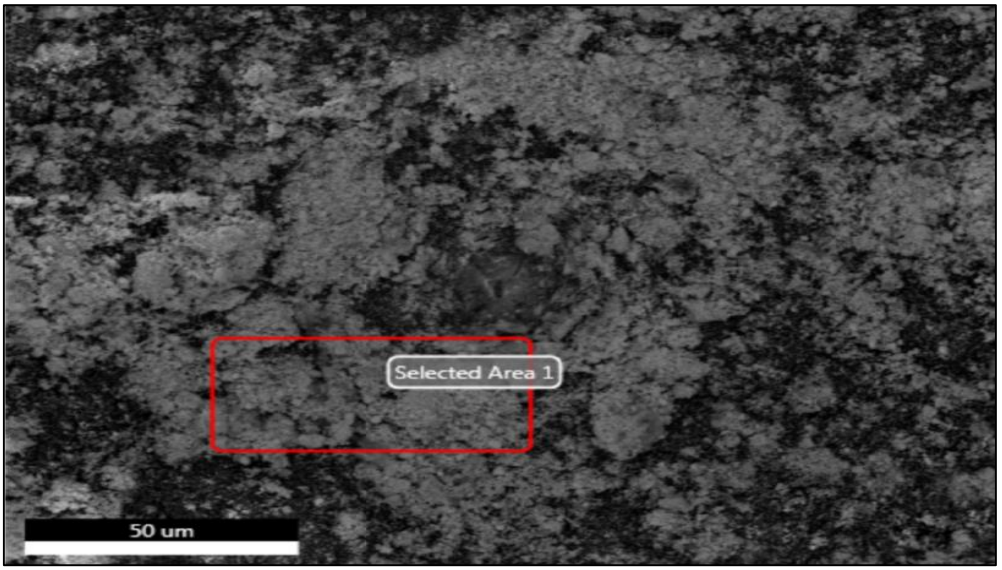

Figure 3. Electron micrographs (STEM) of chemically synthesized ZnO-NPs on 50 microns.

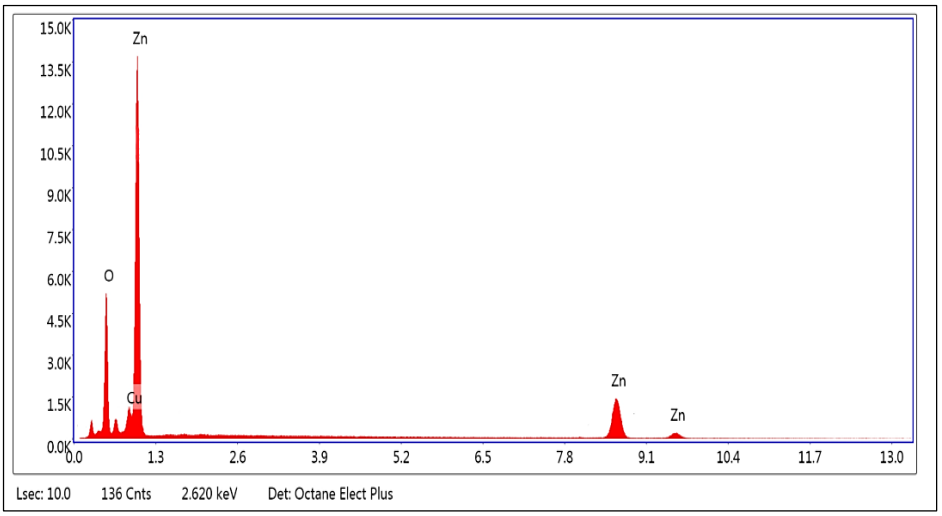

Figure 4. EDAX spectrum of chemically synthesized ZnO-NPs.

Table 3. eZAF Smart Quant results and oxide results.

Element	Weight %	Atomic %
ZnK	67.55	42.95
OxygenK	32.02	56.81
CuK	0.43	0.23

Figure 5 displayed the FTIR spectrum of chemically produced zinc oxide nanoparticles, obtained within the wavelength range from 3900 to 300 cm^{-1}. The spectrum of zinc oxide nanoparticles exhibited peaks corresponding to six functional groups at 3150, 1631.48, 1425.14, 1078.98, 447.404, and 370.23 cm^{-1}.

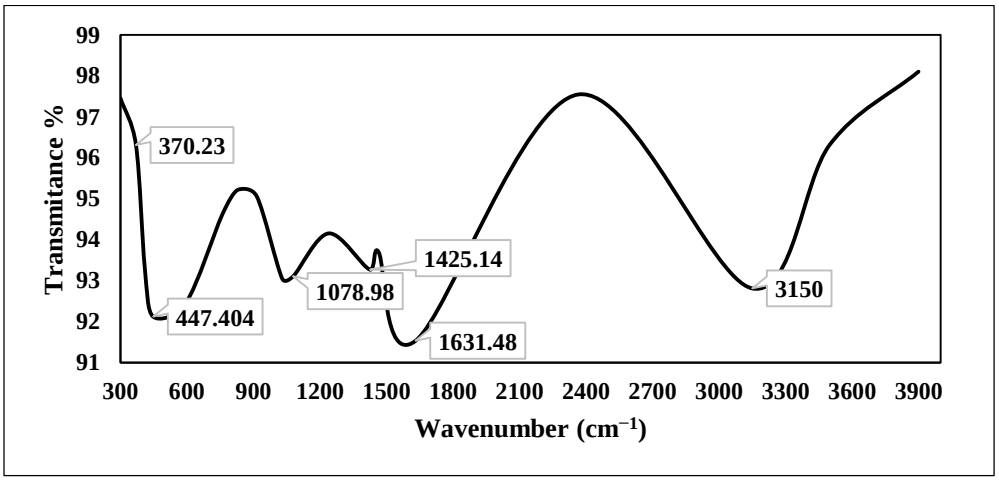

Figure 5. FTIR spectrum of chemically synthesized ZnO-NPs.

Figure 6 displayed the X-ray diffraction (XRD) pattern of chemically generated zinc oxide (ZnO) nanoparticles, both chemically and green. The diffraction peaks were seen at the following angles (2θ): 31.73°, 34.38°, 36.23°, 47.58°, 56.58°, 62.88°, and 76.92°.

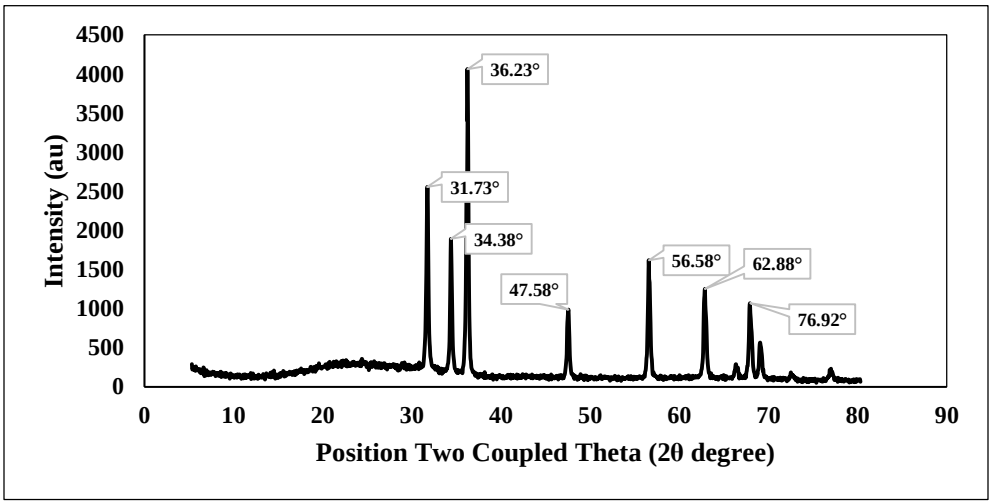

Figure 6. XRD pattern of chemically synthesized ZnO-NPs.

The measured zeta potential was determined to be −30.214 mV, as illustrated in Figure 7.

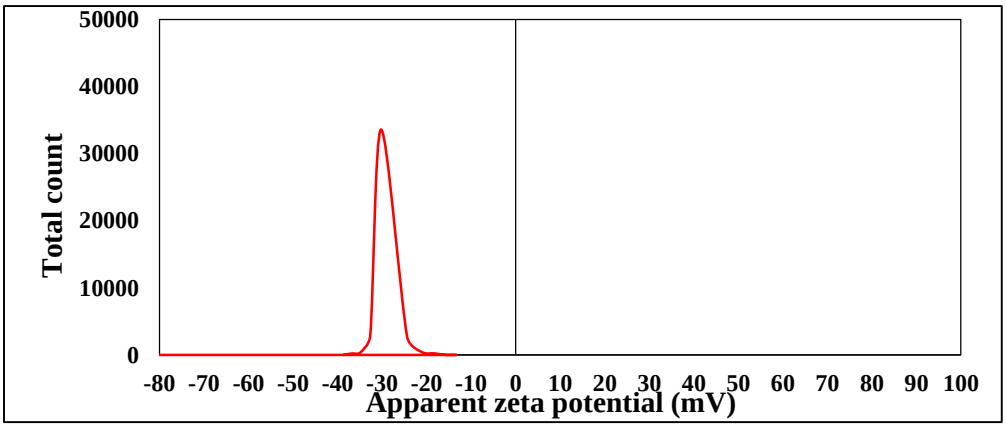

Figure 7. Zeta potential of chemically synthesized ZnO-NPs measuring the charge.

3.2. Determination of different biochemical and stress markers in the leaves from different treatments of tomato and maize

The study analyzed the effects of salt concentrations on tomato and maize leaves (Tables 4 and 5). The results of tomatoes showed that as salt concentrations increased, the total phenolics and flavonoids (TPCs and TFCs), total hydrolyzable sugars, total free amino acids, proline, hydrogen peroxide

(H_2O_2), and malondialdehyde (MDA) contents also increased. The effects of treatments on plant contents of the previous stress and biochemical markers were found to be statistically significant. The fourth stressed treatment (T4) had the highest concentrations of these parameters compared to the two other stressed treatments (T5 and T6), except for protein content. The treatments were sprayed with zinc oxide nanoparticle solutions, controlling the secretion of compounds to ensure compatibility with the initial therapy (control).

The contents of the total phenolics and flavonoids (TPCs and TFCs), hydrolyzable sugars, free amino acids, proline, hydrogen peroxide (H_2O_2), and malondialdehyde (MDA) in the maize leaves all increased as the leaves were exposed to salt. The second treatment (M2) had the highest concentrations of these parameters, except for protein content, which declined to the lowest among the various treatments. The predicted parameter values for the second treatment were in the greatest range compared to the other treatments, regardless of whether they were stressed. The maize experiment was conducted in four combinations: between non-treated (control) and salinity-stressed plants, between non-treated (control) and salinity-stressed plants sprayed with 2 g/L ZnO-NPs, between non-treated and sprayed plants with 2 g/L ZnO-NPs, and between salinity-stressed and salinity-stressed plants sprayed with 2 g/L ZnO-NPs.

Table 4. Determination of the different biochemical and stress markers in the leaves from different treatments of tomato.

Treatments	TPCs (µg/g)	TFCs (µg/g)	Total Hydrolazable Sugars (µg/g)	Total Free Amino Acids (µg/g)	Protein Content (µg/g)	Proline Content (µg/g)	H_2O_2 (µg/g)	MDA (mmols/mL)
T1 Control (dw)	2096 ± 0.10 ^{d}	401 ± 3.39 ^{b}	84.58 ± 4.10 ^{d}	163.73 ± 2.92 ^{f}	81.28 ± 1.16 ^{a}	15.23 ± 0.64 ^{f}	418.76 ± 1.78 ^{e}	1.56 ± 0.077 ^{e}
T2 (dw+ZnO-NPs 75 mg/L)	2829 ± 0.39 ^{bc}	356.56 ± 37.23 ^{b}	107.25 ± 3.43 ^{c}	265.09 ± 5.63 ^{e}	79.11 ± 0.50 ^{ab}	26.90 ± 0.42 ^{e}	571.14 ± 13.33 ^{d}	2.00 ± 0.75 ^{d}
T3 (dw+ZnO-NPs 150 mg/L)	3628 ± 0.50 ^{ab}	362.48 ± 25.98 ^{b}	121.78 ± 4.70 ^{b}	352.59 ± 2.84 ^{d}	78.61 ± 1.13 ^{b}	30.71 ± 1.99 ^{d}	744.00 ± 2.33 ^{b}	2.41 ± 0.094 ^{c}
T4 NaCl (150 mM)	4043 ± 0.44 ^{a}	1191.83 ± 16.66 ^{a}	155.97 ± 0.90 ^{a}	986.68 ± 8.61 ^{a}	26.11 ± 0.33 ^{d}	71.54 ± 2.60 ^{a}	1158.76 ± 11.40 ^{a}	11.77 ±0.24 ^{a}
T5 (150 mM NaCl+ZnO-NPs 75 mg/L)	3730 ± 0.32 ^{ab}	1222.39 ± 62.84 ^{a}	103.22 ± 4.04 ^{c}	694.18 ± 7.24 ^{b}	37.78 ± 0.41 ^{cd}	45.67 ± 1.55 ^{b}	682.57 ± 4.67 ^{c}	2.37 ± 0.08 ^{c}
T6 (150 mM NaCl+ZnO-NPs 150 mg/L)	2596 ± 0.11 ^{c}	1271.37 ± 79.35 ^{a}	121.83 ± 4.04 ^{b}	552.14 ± 3.35 ^{c}	38.89 ± 0.75 ^{c}	41.38 ± 1.91 ^{c}	558.76 ± 7.38 ^{d}	3.55 ± 0.06 ^{b}

Each value represents the mean ± SE. Values with the same letter are not significantly different at ($p \leq 0.05$) (n=4), and the comparison was performed according to different treatments in the same column.

Table 5. Analysis of biochemical and stress indicators in variously treated maize leaves.

Treatments	Concentrations							
	TPCs (mg/g)	TFCs (mg/g)	Total Hydrolazable Sugars (mg/g)	Total Free Amino Acids (mg/g)	Protein Content (mg/g)	Proline Content (mg/g)	H_2O_2 (mg/g)	MDA (mmols/mL)
M1 Control (tap water)	19.99 ± 0.22 ^{c}	18.83 ± 0.07 ^{ab}	177.50 ± 5.60 ^{bc}	53.83 ± 1.23 ^{c}	1.56 ± 0.03 ^{b}	0.22 ± 0.00 ^{b}	1.02 ± 0.01 ^{d}	5.16 ± 0.46 ^{c}
M2 (NaCl 150 mM)	28.42 ± 0.47 ^{a}	19.919 ± 0.06 ^{a}	228.49 ± 2.17 ^{a}	74.35 ± 1.19 ^{a}	0.93 ± 0.01 ^{c}	0.32 ± 0.03 ^{a}	1.78 ± 0.02 ^{a}	13.06 ± 1.61 ^{a}
M3 (NaCl 150 mM + ZnO-NPs 2 g/L)	24.09 ± 0.20 $_{b}$	17.53 ± 0.63 ^{b}	186.31 ± 4.32 ^{b}	56.71 ± 0.72 ^{c}	0.98 ± 0.02 ^{c}	0.31 ± 0.00 ^{a}	1.35 ± 0.03 ^{b}	9.35 ± 0.56 ^{b}
M4 (tap water + ZnO-NPs 2 g/L)	18.61 ± 0.33 ^{d}	17.78 ± 0.11 ^{b}	170.76 ± 2.86 ^{c}	60.83 ± 1.28 ^{b}	2.39 ± 0.03 ^{a}	0.23 ± 0.00 ^{b}	1.19 ± 0.01 ^{c}	5.97 ±0.41 ^{c}

The values indicate the mean is plus or minus the standard error. Superscripted letters indicate if the values are statistically distinguishable at a significance level of $p < 0.05$ or not (n=4). This comparison is made between various treatments within the same column.

3.3. Assessment of the enzymatic activities in tomato and maize leaves

Figure 8 showed the released enzymes: peroxidase (POX), glutathione reductase (GR), glutathione-S-transferase (GST), superoxide dismutase (SOD), and catalase (CAT) **in tomato leaves**. A trend was observed for all released enzymes, where the third non-stressed and sprayed with 75 mg/L ZnO-NPs (T3) had the highest concentration of produced antioxidant enzymes. The plants that were stressed with 150 mM NaCl and sprayed with ZnO-NPs in two different concentrations (T5 and T6); 0.075 and 150 mg/L ZnO-NPs had a higher concentration of produced GR, POX, GST, SOD, and CAT enzymes than the plants that were stressed with NaCl but were not sprayed with the zinc oxide nanoparticles (T4). It was also observed that the plants stressed with sodium chloride and not treated with ZnO-NPs (T4) had the lowest enzyme production values compared to all the other treatments. The second treatment (T2), which was not stressed but treated with ZnO-NPs, resulted in plants with higher values of the produced antioxidative enzymes compared to the control plants that were neither stressed nor sprayed with ZnO-NPs (T1). According to the comparison between the fifth treatment (T5), which was stressed with 150 mM NaCl and sprayed with 75 mg/L ZnO-NPs, and the second treatment, which was not stressed but sprayed, there was a significant difference in the production level of GR and GST, with higher values for the second treatment. On the other hand, the higher values were observed in the fifth treatment plants in the case of SOD. There was minimal variance among the aforementioned interventions in case of POX and CAT.

Figure 9 showed the released enzymes: peroxidase (POX), glutathione reductase (GR), glutathione-S-transferase (GST), superoxide dismutase (SOD), and catalase (CAT) **in maize leaves**. A trend was observed for all released enzymes, where the second stressed and non-sprayed with ZnO-NPs (M2) had the highest concentration of produced antioxidant enzymes. The plants that were stressed with 150 mM NaCl and sprayed with 2 g/L ZnO-NPs (M3); had a higher concentration of produced GR, POX, GST, SOD, and CAT enzymes than the plants that were not stressed with NaCl (control plants) (M1) and also than the plants were not stressed but sprayed with the zinc oxide nanoparticles (M4). It was also observed that the plants were not stressed with sodium chloride and not treated with ZnO-NPs (control plants) (M1) had the lowest enzyme production values compared to all the other treatments. In case of determining the production level of SOD and CAT, there were not any significant differences between the enzymes production according to the plants were sprayed with 2 g /L, however they were stressed with NaCl or not.

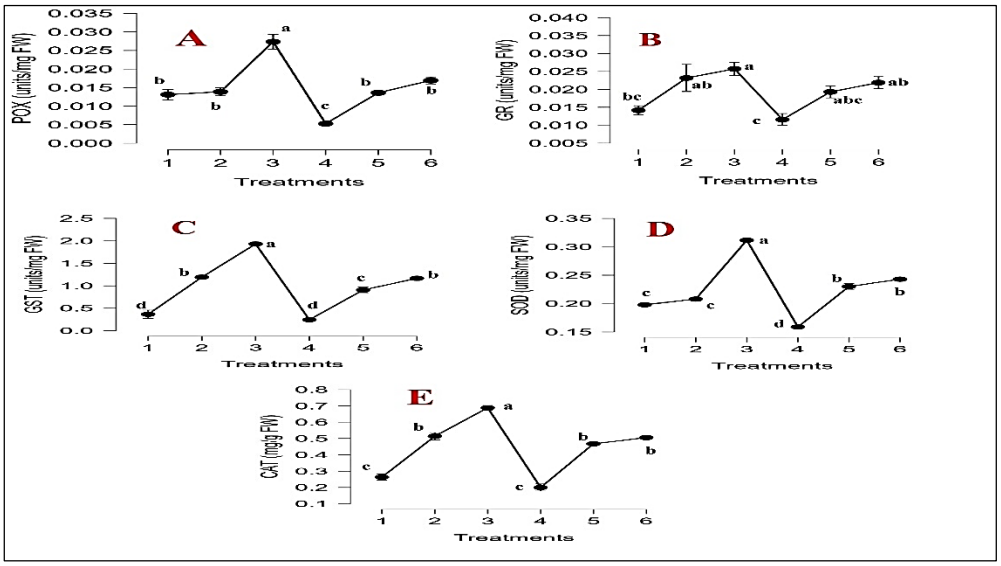

Figure 8. The effects of different treatments on the concentration of peroxidase (POX) (**A**), glutathione reductase (GR) (**B**), glutathione-S-transferase (GST) (**C**), superoxide dismutase (SOD) (**D**), and catalase (CAT) (**E**) enzymes in tomato leaves.
1*: T1; control (dw);* ***2****: T2; dw+ZnO-NPs 75 mg/L;* ***3****: T3; dw+ZnO-NPs 150 mg/L;* ***4****: T4; NaCl (150 mM);* ***5****: T5; 150 mM NaCl+ZnO-NPs 75 mg/L; and* ***6****: T6; 150 mM NaCl+ZnO-NPs 150 mg/L. The mean plus or minus the standard error is what each value stands for. The small letters above the bars show how significant the results are. If they have the same letter over values, it means they are not statistically different (p < 0.05) (n=4).*

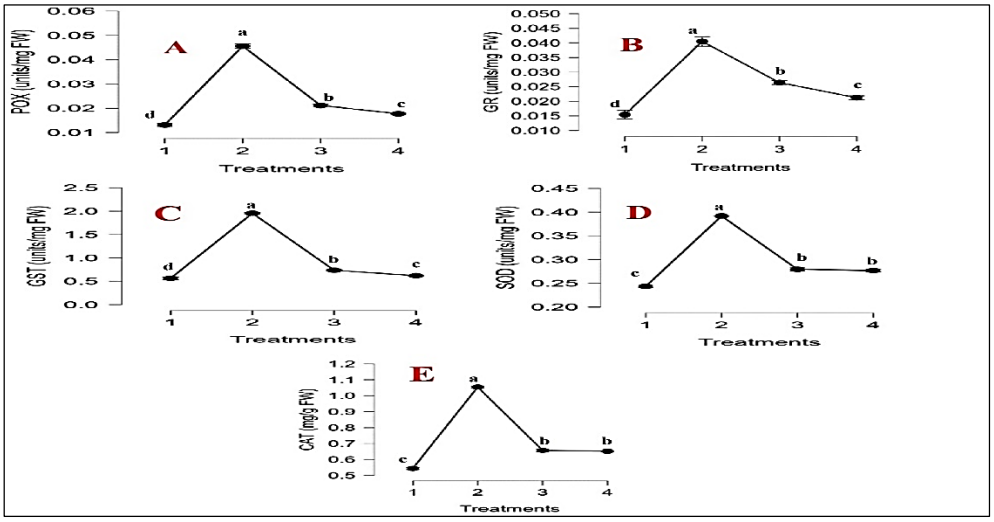

Figure 9. The effects of different treatments on the concentration of peroxidase (POX) (**A**), glutathione reductase (GR) (**B**), glutathione-S-transferase (GST) (**C**), superoxide dismutase (SOD) (**D**), and catalase (CAT) (**E**) enzymes in mazie leaves.
1*: M1; Control (tap water);* ***2****: M2; (NaCl 150 mM);* ***3****: M3; (NaCl 150 mM + ZnO-NPs 2 g/L); and* ***4****: M4; (tap water + ZnO-NPs 2 g/L).The mean plus or minus the standard error is what each value stands for. The small letters above the bars show how significant the results are. If they have the same letter over values, it means they are not statistically different (p < 0.05) (n=4).*

3.4. Genome-wide transcriptomic analyses

Total raw reads (post-sequencing) of the different treatments in **tomato** varied between 40,332,114 and 63,450,658. The raw reads measured 151 bp in length, the total count of contigs after *de novo* assembling was 87,567, and the mean length of the contigs was 1,176 bp (Ahmed et al., 2025). The comprehensive super transcriptome (Transcriptome Shotgun Assembly – TSA) serves as a depository of programmatically assembled transcript sequences obtained from primary sources of data, such as archived raw sequencing data (SRAs) and next-generation sequencing.

Overlapping reads from the entire transcriptome were computationally reconstructed into transcripts (*in silico*). The data underwent blasting, mapping, and annotation, subsequently followed by RNA sequencing read quantification to determine the level of expression of the *de novo* transcriptome contigs. This was crucial since differential expression analysis requires the assessment of individual degrees of expression of the contigs.

The top 50 up- and down-differentially expressed contigs involved in the pairwise differential analysis between treatments were identified, as shown in the heat maps (Figures 10-16).

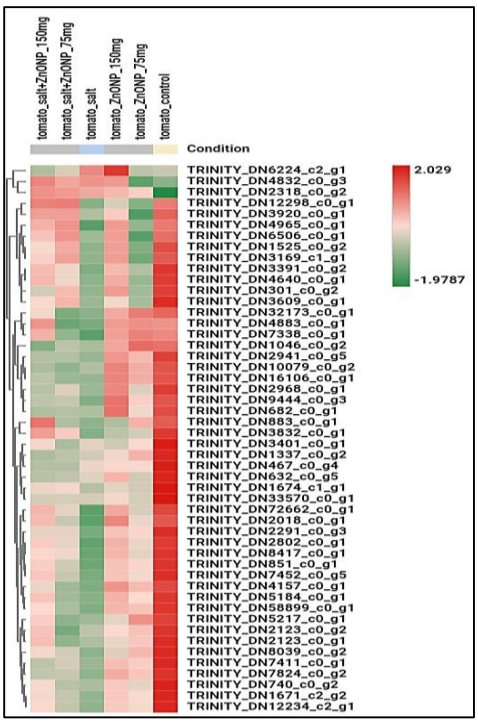

Figure 10. Comparative transcriptome analysis of control vs. salinity-stressed treatments. Up-regulated and down-regulated DEGs are observed in red and green, respectively.

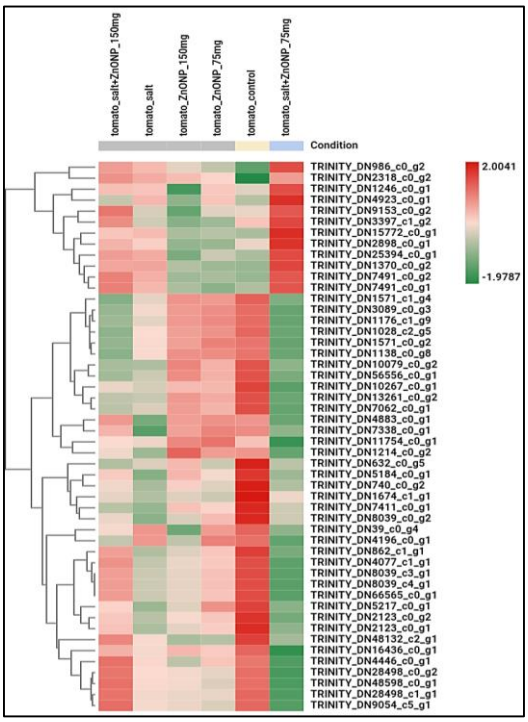

Figure 11. Comparative transcriptome analysis of control vs. 75 mg/L ZnO-NPs sprayed treatments. Up-regulated and down-regulated DEGs are observed in red and green, respectively.

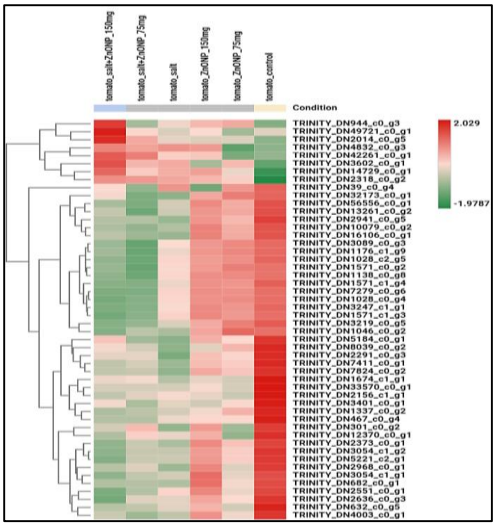

Figure 12. Comparative transcriptome analysis of control vs. 150 mg/L ZnO-NPs sprayed treatments. Up-regulated and down-regulated DEGs are observed in red and green, respectively.

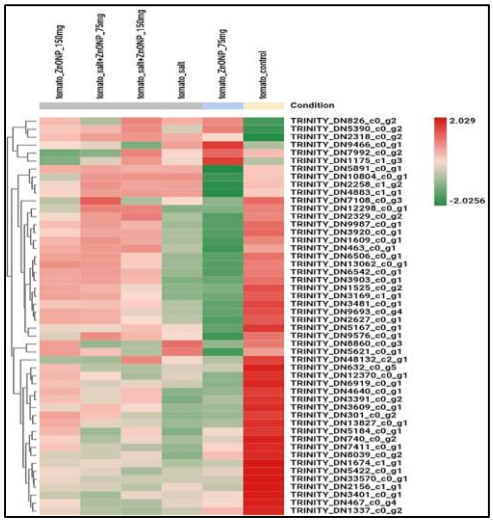

Figure 13. Comparative transcriptome analysis of control vs. salinity-stressed and 75 mg/L ZnO-NPs sprayed treatments. Up-regulated and down-regulated DEGs are observed in red and green, respectively.

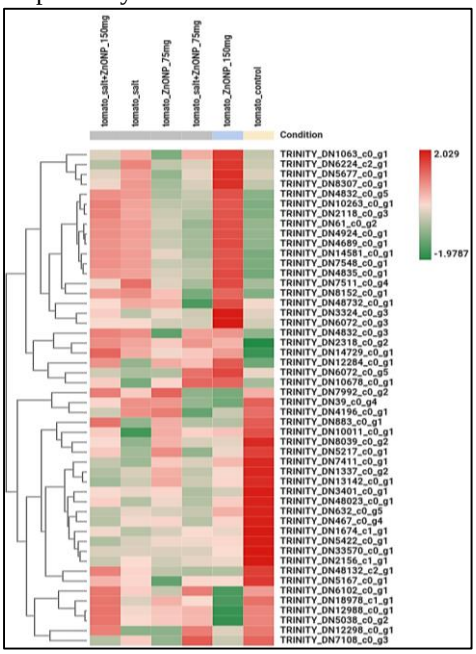

Figure 14. Comparative transcriptome analysis of control vs. salinity-stressed and 150 mg/L ZnO-NPs sprayed treatments. Up-regulated and down-regulated DEGs are observed in red and green, respectively.

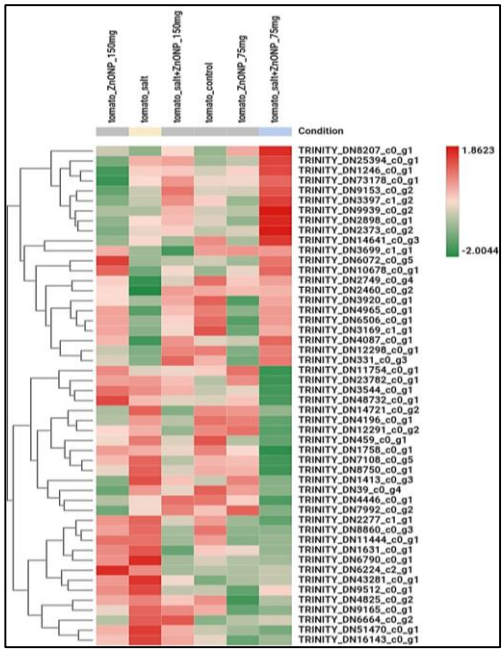

Figure 15. Comparative transcriptome analysis of salinity-stressed vs. salinity-stressed + 75 mg/L ZnO-NPs sprayed treatments. Up-regulated and down-regulated DEGs are observed in red and green, respectively.

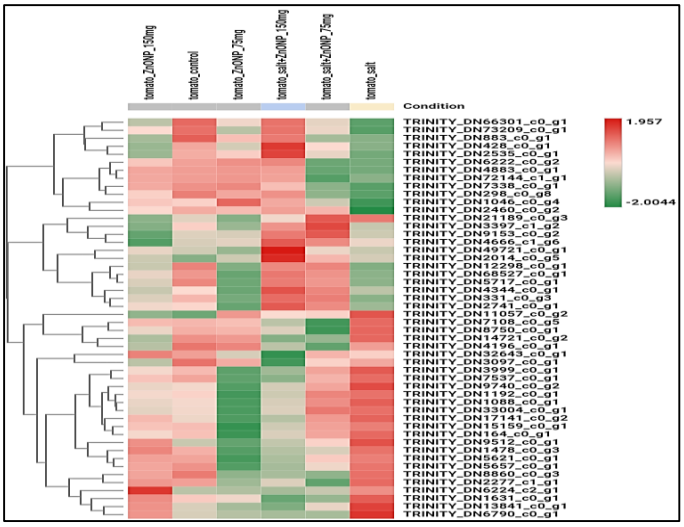

Figure 16. Comparative transcriptome analysis of salinity-stressed vs. salinity-stressed + 150 mg/L ZnO-NPs sprayed treatments. Up-regulated and down-regulated DEGs are observed in red and green, respectively.

The raw reads of maize measured 201 bp in length; the total count of contigs after *de novo* assembling was 22,108. The total assembled bases were varied between 6,174,394 and 7,623,144, and the mean length of the contigs was 348 bp. The comprehensive super transcriptome (Transcriptome Shotgun Assembly – TSA) serves as a depository of programmatically assembled transcript sequences obtained from primary sources of data, such as archived raw sequencing data (SRAs) and next-generation sequencing. Overlapping reads from the entire transcriptome were computationally reconstructed into transcripts (*in silico*). This was crucial since differential expression analysis requires the assessment of individual degrees of expression of the contigs.

Heat maps can be used to visualize the gene expression across samples. The top 50 up- and down-differentially expressed contigs involved in the pairwise differential analysis between treatments were identified, as shown in the heat maps (Figures 17-20).

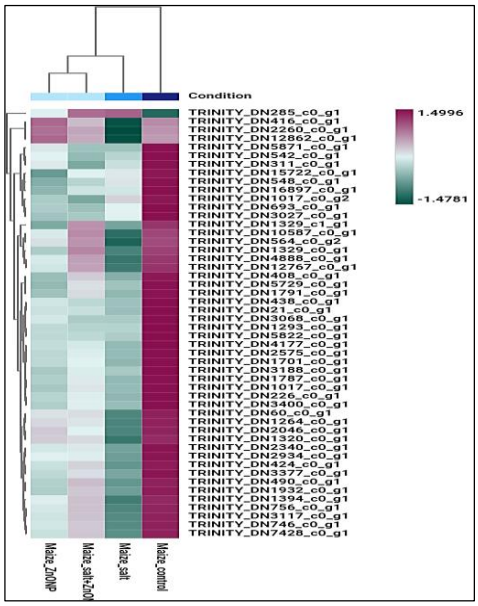

Figure 17. Comparative transcriptome analysis of control vs. salinity-stressed treatments. Up-regulated and down-regulated DEGs are observed in red and green, respectively.

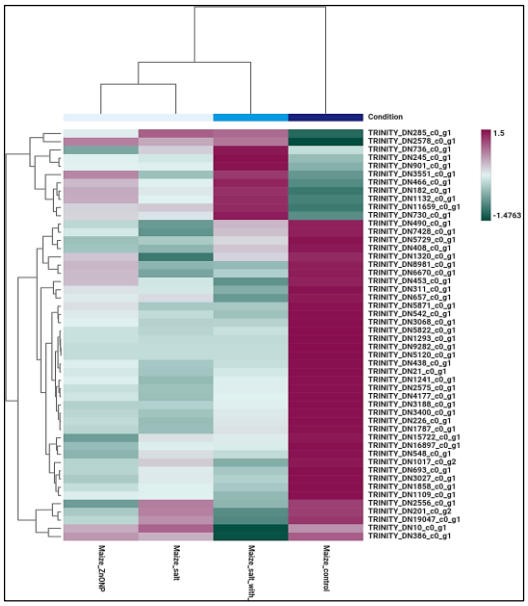

Figure 18. Comparative transcriptome analysis of control vs. salinity-stressed and 2 g/L ZnO-NPs sprayed treatments. Up-regulated and down-regulated DEGs are observed in red and green, respectively.

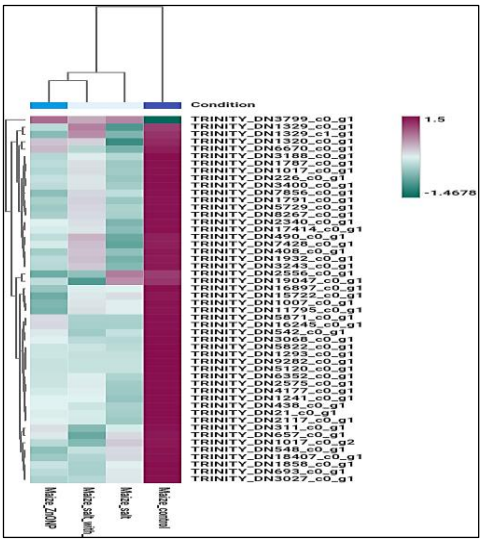

Figure 19. Comparative transcriptome analysis of control vs. 2 g/L ZnO-NPs sprayed treatments. Up-regulated and down-regulated DEGs are observed in red and green, respectively.

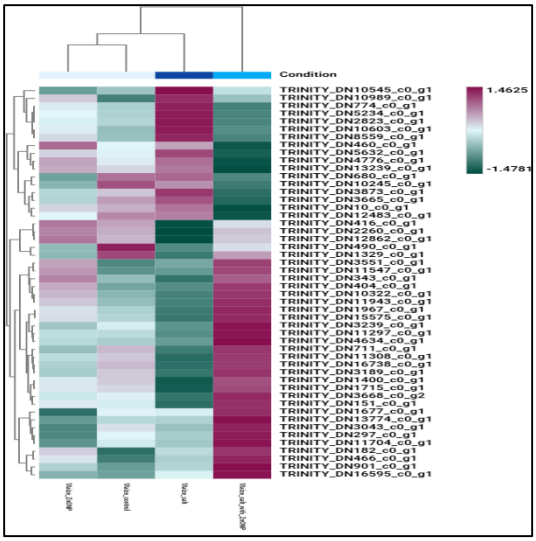

Figure 20. Comparative transcriptome analysis of salinity-stressed vs. salinity-stressed + 2 g/L ZnO-NPs sprayed treatments. Up-regulated and down-regulated DEGs are observed in red and green, respectively.

3.5. Determination of the antimicrobial activities of the aqueous and diethyl ether extracts from tomato and maize leaves

For tomato samples, as illustrated in Table 6, the aqueous extract of different treatments exhibited minimum inhibitory concentration (MIC) values within the range of 1.08 to 0.42 mg/mL against *Staph. aureus*, and the most potent activity with the lowest MIC value of 0.42 mg/mL resulted from T6 aqueous extract. No notable distinction was observed among various treatments concerning the following pathogenic bacteria: *B. cereus*, *E. coli*, and *L. monocytogenes*. The lowest MIC values against *S. typhi* resulted from T1, T2, and T5 aqueous extracts with 0.15, 0.2, and 0.2 mg/mL, respectively. While T3 aqueous extract had the highest activity (lowest MIC) against *P. aeruginosa*. Table 7 shows the MIC results of the diethyl ether extracts from different treatments against the food-borne pathogenic bacteria. In case of *B. cereus*, the diethyl ether extract from T6 showed the highest effect with 0.41 mg/mL. *Staph. aureus* was highly affected by the diethyl ether extract from T2, followed by T1 with 0.2 and 0.33 mg/L. T3 extract showed the lowest MIC value against *L. monocytogenes* with 0.33 mg/mL, while T1 extract had the highest effect against *E. coli* with 0.2 mg/mL. For *S. typhi* and *P. aeruginosa*, they were highly affected by the extracts of T1 with 0.15 and 0.58 mg/mL, compared to the other treatment extracts.

Table 6. Minimum inhibitory concentration (mg/mL) of tomato leaf aqueous extracts against pathogenic bacteria.

Bacteria	T1	T2	T3	T4	T5	T6
B. cereus	0.15±0.08 ^{a}	0.33±0.12 ^{a}	0.07±0.08 ^{a}	0.28±0.18 ^{a}	0.42±0.13 ^{a}	0.33±0.12 ^{a}
Staph. aureus	0.67±0.12 ^{ab}	0.75±0.22 ^{ab}	1.08±0.12 ^{a}	0.67±0.12 ^{ab}	0.83±0.25 ^{ab}	0.42±0.25 ^{b}
L. monocytogenes	0.1±0.00^{a}	0.15±0.0 ^{a}	0.2±0.08^{a}	0.28±0.20 ^{a}	0.37±0.23 ^{a}	0.2±0.08^{a}
E. coli	0.58±0.12 ^{a}	0.83±0.12 ^{a}	0.58±0.34 ^{a}	0.42±0.12 ^{a}	0.33±0.12 ^{a}	0.42±0.12 ^{a}
S. typhi	0.15±0.08 ^{b}	0.2±0.08^{b}	0.42±0.12 ^{ab}	0.5±0.22^{ab}	0.2±0.08^{b}	0.67±0.12 ^{a}
P. aeruginosa	0.42±0.12 ^{ab}	0.58±0.12 ^{ab}	0.33±0.12 ^{b}	0.42±0.12 ^{ab}	0.83±0.12 ^{a}	0.5±0.22^{a} ^{b}

Each value represents the mean ± SE (n=4). The lower-case letters above the values indicate the significance level. The same letter over values denotes that they are not significantly different at ($p \leq 0.05$), and comparison is performed according to each strain with all samples (confidence intervals corrected using Tukey method). ***T1****: Control (non-treated) (dw).* ***T2****: (dw + ZnO-NPs 75 mg/L).* ***T3****: (dw + ZnO-NPs 150 mg/L).* ***T4****: NaCl (150 mM).* ***T5****: (150 mM NaCl + ZnO-NPs 75 mg/L).* ***T6****: (150 mM NaCl + ZnO-NPs 150 mg/L).*

Table 7. Minimum inhibitory concentration (mg/mL) of tomato leaf diethyl ether extracts against pathogenic bacteria.

Bacteria	T1	T2	T3	T4	T5	T6
B. cereus	1.0±0.22^{a}	0.92±0.12^{ab}	0.83±0.12^{ab}	0.67±0.12^{ab}	0.58±0.08^{ab}	0.41±0.05^{b}
Staph. aureus	0.33±0.12^{b}	0.2±0.08^{b}	0.92±0.12^{a}	0.58±0.25^{ab}	0.5±0.22^{ab}	0.58±0.12^{ab}
L. monocytogenes	0.83±0.12^{ab}	0.58±0.12^{ab}	0.33±0.08^{b}	0.92±0.25^{a}	0.58±0.12^{ab}	0.67±0.25^{ab}
E. coli	0.2±0.08^{b}	0.67±0.28^{ab}	0.92±0.12^{a}	1.08±0.28^{a}	0.67±0.14^{ab}	0.58±0.14^{ab}
S. typhi	0.15±0.08^{c}	0.42±0.12^{bc}	1.08±0.11^{a}	1.0±0.22^{ab}	1.08±0.26^{a}	0.92±0.34^{ab}
P. aeruginosa	0.58±0.12^{b}	0.83±0.11^{ab}	0.67±0.12^{b}	0.58±0.08^{b}	1.08±0.12^{a}	0.92±0.12^{ab}

Each value represents the mean ± SE (n=4). The lower-case letters above the values indicate the significance level. The same letter over values denotes that they are not significantly different at ($p \leq 0.05$), and comparison is performed according to each strain with all samples (confidence intervals corrected using Tukey method). ***T1****: Control (non-treated) (dw).* ***T2****: (dw + ZnO-NPs 75 mg/L).* ***T3****: (dw + ZnO-NPs 150 mg/L).* ***T4****: NaCl (150 mM).* ***T5****: (150 mM NaCl + ZnO-NPs 75 mg/L).* ***T6****: (150 mM NaCl + ZnO-NPs 150 mg/L).*

As illustrated in Table 8, the aqueous extract of different treatments exhibited the most potent activity with the lowest MIC value of 0.33 mg/mL, resulting from T2 aqueous extract, followed by T5 extract with 0.42 mg/mL against *A. flavus*. T1 aqueous extract had the highest activity against *A. niger* with 0.2 mg/mL, while *A. carbonarius* was highly affected by T2 and T1 extracts, with 0.15 mg/mL for both. T5 extract had the highest activity with the lowest MIC against *A. ochraceus* with 0.28 mg/mL. For *F. verticilioides* and *F. proliferatium*, both were highly affected by T1 aqueous extract with 0.58 mg/mL from both extracts. Table 9 shows the MIC results of the diethyl ether extracts from different treatments against the mycotoxigenic fungi. T2 diethyl ether extract had the highest activity against *A. flavus* with 0.33 mg/mL, while the same extract had also the highest effect against *A. niger* with 0.58 mg/mL compared to the other treatment extracts. *A. carbonarius* was highly affected by T1 extract with 0.58 mg/mL, and for *A. ochraceus*, extracts of T1, T3, T4, and T5 had the lowest MICs within the range of 0.58 to 0.67 mg/mL. For *F. verticilioides* and *F. proliferatium*, both were highly affected by T1 aqueous extract with 0.58 and 0.33 mg/mL, respectively.

Table 8. Minimum inhibitory concentration (mg/mL) of tomato leaf aqueous extracts against mycotoxigenic fungi.

Fungi	T1	T2	T3	T4	T5	T6
A. flavus	0.58±0.12 bc	0.33±0.04 c	1.08±0.11 a	0.67±0.12 b c	0.42±0.08 c	0.83±0.12 ab
A. niger	0.2±0.07 c	0.42±0.08 bc	0.67±0.13 a bc	0.58±0.11 a bc	0.92±0.12 a	0.83±0.15 ab
A. carbonarius	0.15±0.08 c	0.15±0.07 c	0.67±0.15 a bc	0.28±0.08 b c	0.83±0.15 ab	1.00±0.22 a
A. ochraceus	0.67±0.14 ab	0.58±0.14 ab	0.67±0.18 a b	0.83±0.14 a	0.28±0.10 b	0.83±0.14 a
F. verticilioides	0.58±0.12 c	1.08±0.08 bc	1.33±0.25 b	1.42±0.12 b	2.16±0.25 a	1.25±0.22 b
F. proliferatium	0.58±0.05 c	0.83±0.12 bc	1.16±0.12 a b	1.42±0.12 a	1.17±0.13 ab	1.33±0.12 a

Each value represents the mean ± SE (n=4). The lower-case letters above the values indicate the significance level. The same letter over values denotes that they are not significantly different at ($p \leq 0.05$), and comparison is performed according to each strain with all samples (confidence intervals corrected using Tukey method). ***T1****: Control (non-treated) (dw).* ***T2****: (dw + ZnO-NPs 75 mg/L).* ***T3****: (dw + ZnO-NPs 150 mg/L).* ***T4****: NaCl (150 mM).* ***T5****: (150 mM NaCl + ZnO-NPs 75 mg/L).* ***T6****: (150 mM NaCl + ZnO-NPs 150 mg/L).*

Table 9. Minimum inhibitory concentration (mg/mL) of tomato leaf diethyl ether extracts against mycotoxigenic fungi.

Fungi	T1	T2	T3	T4	T5	T6
A. flavus	0.67±0.12 a b	0.33±0.08 b	1.08±0.12 a	0.58±0.12 a b	0.75±0.22 a b	0.92±0.14 a b
A. niger	1.33±0.15 a	0.58±0.08 c	0.83±0.12b c	0.67±0.11 c	1.08±0.12 a b	0.92±0.13 bc
A. carbonarius	0.58±0.08 b	0.67±0.12 a b	1.08±0.13 a	0.67±0.08 a b	0.83±0.12 a b	1.0±0.12 ab
A. ochraceus	0.67±0.12 b	0.75±0.15 a b	0.67±0.14 b	0.58±0.08 b	0.67±0.12 b	1.16±0.14 a
F. verticilioides	0.58±0.12 d	0.67±0.11 c d	1.16±0.12 bc	1.33±0.25 b	1.33±0.13 b	2.33±0.25 a
F. proliferatium	0.33±0.08 b	0.58±0.12 a b	0.75±0.22 a b	0.67±0.11 a b	0.83±0.12 a b	1.0±0.22 a

Each value represents the mean ± SE (n=4). The lower-case letters above the values indicate the significance level. The same letter over values denotes that they are not significantly different at ($p \leq 0.05$), and comparison is performed according to each strain with all samples (confidence intervals corrected using Tukey method). ***T1****: Control (non-treated) (dw).* ***T2****: (dw + ZnO-NPs 75 mg/L).* ***T3****: (dw + ZnO-NPs 150 mg/L).* ***T4****: NaCl (150 mM).* ***T5****: (150 mM NaCl + ZnO-NPs 75 mg/L).* ***T6****: (150 mM NaCl + ZnO-NPs 150 mg/L).*

For maize samples, as illustrated in Table 10, the aqueous extract of different treatments exhibited minimum inhibitory concentration (MIC) values within the range of 1.08 to 0.67 mg/mL against *L. monocytogenes*, and the most potent activity with the lowest MIC value of 0.67 mg/mL resulted from M3 aqueous extract. No notable distinction was observed among various

treatments concerning the following pathogenic bacteria: *B. cereus*, *Staph. aureus*, *E. coli*, and *P. aeruginosa.* The lowest MIC values against *S. typhi* resulted from M3 and M4 aqueous extracts with 0.92, and 0.83 mg/mL, respectively. Table 11 shows the MIC results of the diethyl ether extracts from different treatments against the pathogenic bacteria. M3 aqueous extract had the highest activity (lowest MIC) against *S. typhi* with 0.20 mg/mL. In case of *B. cereus*, *Staph. aureus*, and *P. aeruginosa* the diethyl ether extracts showed no notable distinction was observed among various treatments. M4 extract showed the lowest MIC value against *E. coli* with 0.33 mg/mL, while for *L. monocytogenes*, it was highly affected by the extract of M4 with 0.15 mg/mL, compared to the other treatment extracts.

Table 10. The minimal concentration (mg/mL) inhibiting the different bacterial strains using the maize leaf aqueous extracts.

Bacteria	M1	M2	M3	M4
B. cereus	0.58 ± 0.13^{a}	0.67 ± 0.13^{a}	0.58 ± 0.13^{a}	0.33 ± 0.13^{a}
Staph. aureus	1.25 ± 0.22^{a}	0.92 ± 0.13^{a}	0.83 ± 0.13^{a}	0.92 ± 0.13^{a}
L. monocytogenes	1.08 ± 0.14^{a}	0.83 ± 0.14^{ab}	0.67 ± 0.14^{ab}	0.92 ± 0.29^{b}
E. coli	1.83 ± 0.26^{a}	1.67 ± 0.26^{a}	1.58 ± 0.34^{a}	0.92 ± 0.13^{a}
S. typhi	1.67 ± 0.29^{a}	1.17 ± 0.26^{ab}	0.92 ± 0.13^{b}	0.83 ± 0.13^{b}
P. aeruginosa	1.83 ± 0.26^{a}	2.17 ± 0.26^{a}	2.33 ± 0.26^{a}	1.67 ± 0.26^{a}

Each value represents the mean ± SE (n=4). The significance of the numbers is shown by the lowercase letters that appear above them. Two values are not substantially different ($p < 0.05$) if they share a letter. All samples were statistically compared to each item (confidence intervals corrected using Tukey method). ***M1****: Control (tap water);* ***M2****: (NaCl 150 mM);* ***M3****: (NaCl 150 mM + ZnO-NPs 2 g/L); and* ***M4****: (tap water + ZnO-NPs 2 g/L).*

Table 11. The minimal concentration (mg/mL) inhibiting the different bacterial strains using the maize leaf diethyl ether extracts.

Bacteria	M1	M2	M3	M4
B. cereus	0.20 ± 0.08^{a}	0.15 ± 0.08^{a}	0.20 ± 0.08^{a}	0.23 ± 0.21^{a}
Staph. aureus	0.37 ± 0.21^{a}	0.58 ± 0.13^{a}	0.67 ± 0.13^{a}	0.58 ± 0.13^{a}
L. monocytogenes	0.83 ± 0.13^{a}	0.33 ± 0.13^{ab}	0.42 ± 0.13^{ab}	0.15 ± 0.08^{b}
E. coli	0.83 ± 0.14^{a}	0.58 ± 0.14^{b}	0.50 ± 0.25^{b}	0.33 ± 0.14^{b}
S. typhi	0.58 ± 0.13^{a}	0.42 ± 0.13^{ab}	0.20 ± 0.08^{b}	0.15 ± 0.08^{b}
P. aeruginosa	1.17 ± 0.26^{a}	1.33 ± 0.26^{a}	1.17 ± 0.26^{a}	0.67 ± 0.13^{a}

Each value represents the mean ± SE (n=4). The significance of the numbers is shown by the lowercase letters that appear above them. Two values are not substantially different ($p < 0.05$) if they share a letter. All samples were statistically compared to each item (confidence intervals corrected using Tukey method). ***M1****: Control (tap water);* ***M2****: (NaCl 150 mM);* ***M3****: (NaCl 150 mM + ZnO-NPs 2 g/L); and* ***M4****: (tap water + ZnO-NPs 2 g/L).*

As illustrated in Table 12, the aqueous extract of different treatments exhibited minimum inhibitory concentration (MIC) values within the range of 1.67 to 0.83 mg/mL against *F. verticilloids*, and the most potent activity with the lowest MIC value of 0.83 mg/mL resulted from M2 aqueous extract. No notable distinction was observed among various treatments concerning the

following fungi: *A. niger*, *A. flavus*, *A. ochraceus*, *F. proliferatum*, and *P. vercosum*. As illustrated in Table 13, the aqueous extract of different treatments exhibited minimum inhibitory concentration (MIC) values within the range of 1.17 to 0.14 mg/mL against *A. flavus*, and the most potent activity with the lowest MIC value of 0.14 mg/mL resulted from M3 aqueous extract. No notable distinction was observed against *A. niger* according to all the treatments. For *A. ochraceus*, the lowest MIC which represented the highest activity was obtained from M2, M3, and M4 with 0.75, 0.14, and 0.42 mg/mL, respectively. While *F. proliferatum*, and *P. vercosum* were highly affected by the M3 and M4 extracts with 0.14 and 0.20 mg/mL for the first, 0.14 and 0.58 mg/mL for the second, respectively, and no significant differences were obtained at the effect of M1 and M2 extracts against both fungi.

Table 12. The minimal concentration (mg/mL) inhibiting the different fungal strains using the maize leaf aqueous extracts.

Fungi	M1	M2	M3	M4
A. flavus	1.83±0.58^{a}	1.25±0.25^{a}	1.33±0.29^{a}	1.83±0.29^{a}
A. niger	1.58±0.38^{a}	1.17±0.14^{a}	1.58±0.38^{a}	0.83±0.14^{a}
A. ocheraceus	1.67±0.29^{a}	1.67±0.76^{a}	1.17±0.14^{a}	0.92±0.14^{a}
F. profileratum	1.08±0.14^{a}	0.92±0.14^{a}	4.08±5.34^{a}	1.00±0.25^{a}
F. verticilloids	1.33±0.29^{ab}	0.83±0.14^{b}	1.50±0.43^{ab}	1.67±0.29^{a}
P. vercosum	1.67±1.04^{a}	2.17±0.29^{a}	1.33±0.29^{a}	1.83±0.29^{a}

Each value represents the mean ± SE (n=4). The significance of the numbers is shown by the lowercase letters that appear above them. Two values are not substantially different ($p < 0.05$) if they share a letter. All samples were statistically compared to each item (confidence intervals corrected using Tukey method). ***M1****: Control (tap water);* ***M2****: (NaCl 150 mM);* ***M3****: (NaCl 150 mM + ZnO-NPs 2 g/L); and* ***M4****: (tap water + ZnO-NPs 2 g/L).*

Table 13. The minimal concentration (mg/mL) inhibiting the different fungal strains using the maize leaf diethyl ether extracts.

Fungi	M1	M2	M3	M4
A. flavus	1.08±0.14^{ab}	1.17±0.29^{a}	0.92±0.14^{a}	0.67±0.14^{b}
A. niger	0.83±0.29^{a}	0.83±0.14^{a}	0.58±0.14^{b}	0.67±0.29^{a}
A. ocheraceus	1.33±0.14^{a}	0.75±0.25^{b}	0.58±0.14^{b}	0.42±0.29^{b}
F. profileratum	0.67±0.14^{a}	0.58±0.14^{a}	0.33±0.14^{b}	0.20±0.09^{b}
F. verticilloids	0.83±0.14^{a}	1.08±0.14^{a}	0.83±0.14^{ab}	0.42±0.14^{b}
P. vercosum	0.92±0.14^{ab}	1.08±0.14^{a}	0.83±0.14^{ab}	0.58±0.14^{b}

Each value represents the mean ± SE (n=4). The significance of the numbers is shown by the lowercase letters that appear above them. Two values are not substantially different ($p < 0.05$) if they share a letter. All samples were statistically compared to each item (confidence intervals corrected using Tukey method). ***M1****: Control (tap water);* ***M2****: (NaCl 150 mM);* ***M3****: (NaCl 150 mM + ZnO-NPs 2 g/L); and* ***M4****: (tap water + ZnO-NPs 2 g/L).*

3.6. Molecular docking results

In case of phenolic compounds detected in tomato, the interaction of 07N original ligand, caffeic acid, ferulic acid, and *p*-coumaric acid within DNA Gyrase's active site (as antibacterial targets) has been investigated and illustrated in both two and three dimensions, as shown in Figure 21a, 21b, 21c, and 21d, respectively, and the interaction between the original ligand (X2N), ferulic acid, sinapic acid, and Apigenin-7-glucoside.within the active site of CYP51 (as antifungal targets) has been studied and visualized (2D and 3D) in Figure 22a, 22b, 22c, and 22d, respectively.

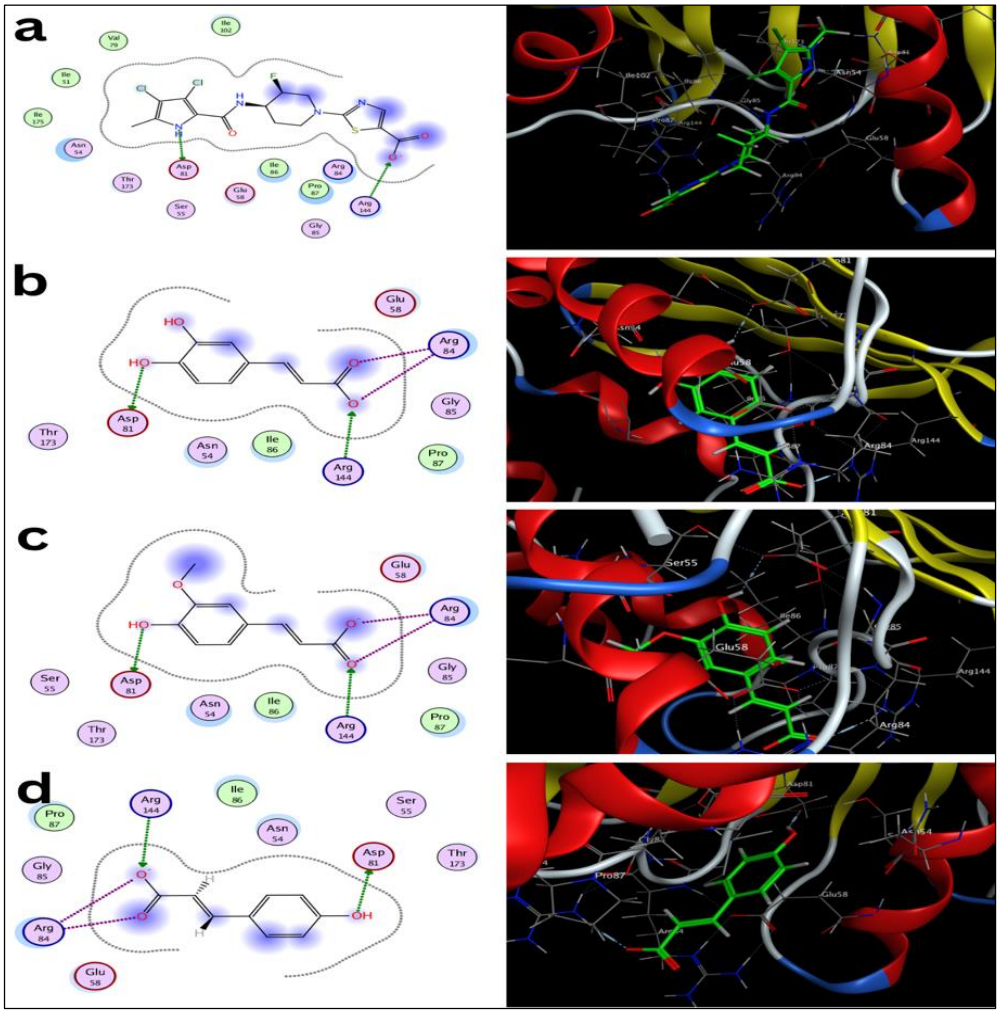

Figure 21. Selected 2D and 3D visualizations of the projected interaction modes and mechanisms of binding between studied compounds and DNA Gyrase Enzyme's active site.
(a) *original ligand 07N,* ***(b)*** *Caffeic acid,* ***(c)*** *Ferulic acid,* ***(d)*** *p-coumaric acid.*

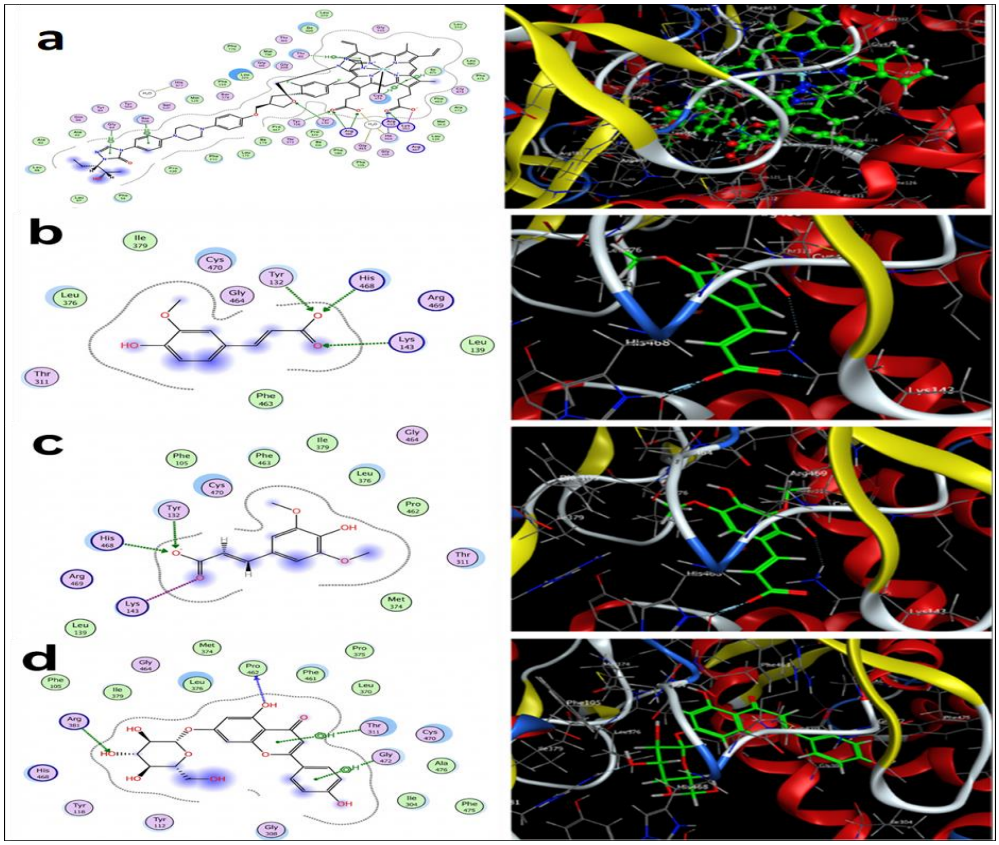

Figure 22. Selected 2D and 3D illustrations of the projected interaction modes and mechanisms of binding between the studied compounds and the sterol 14-alpha demethylase (CYP51) enzyme active site.
(a) *Original ligand,* ***(b)*** *Ferulic acid,* ***(c)*** *Sinapic acid,* ***(d)*** *Apigenin-7-glucoside.*

The interaction of original ligand CWW, Rutin, Apeginin-7-glucoside, and clorogenic acid within DNA Gyrase's active site (as antibacterial targets) has been investigated and illustrated in both two and three dimensions, as shown in Figure 23a, 23b, 23c, and 23d, respectively. Similarly, the interaction between the original ligand (NAG), rutin, apeginin-7-glucoside, and clorogenic acid within the active site of alpha−L−fucosidase enzyme has been investigated and illustrated in both two and three dimensions, as shown in Figure 24a, 24b, 24c, and 24d, respectively.

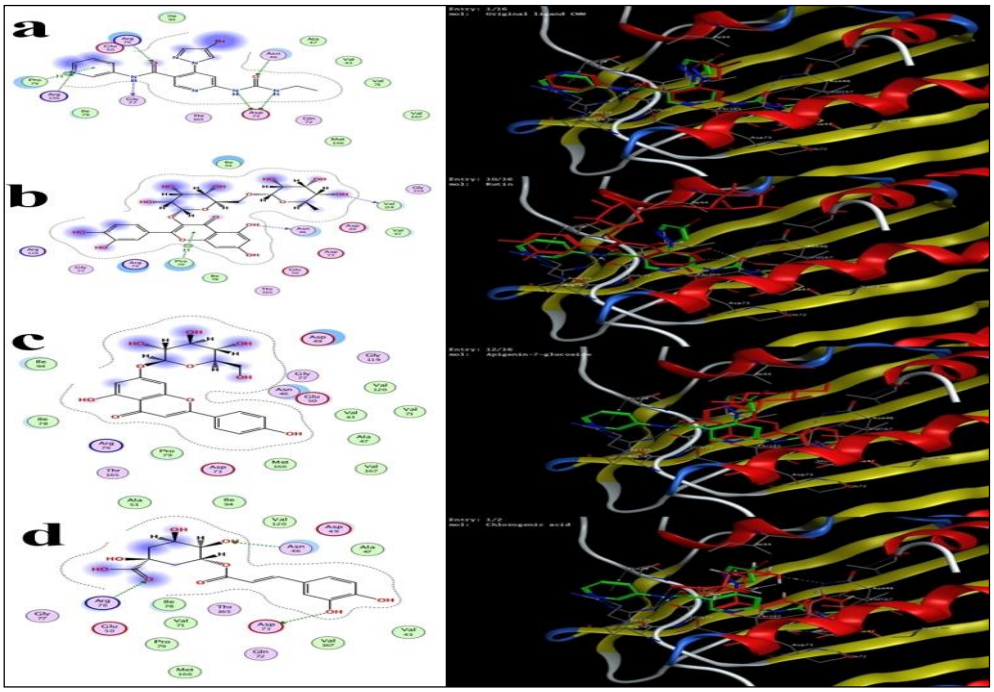

Figure 23. Selected 2D and 3D visualizations of the projected interaction modes and mechanisms of binding between studied compounds and DNA Gyrase Enzyme's active site.
*(**a**) original ligand CWW, (**b**) Rutin, (**c**) Apeginin-7-glucoside, (**d**) clorogenic acid.*

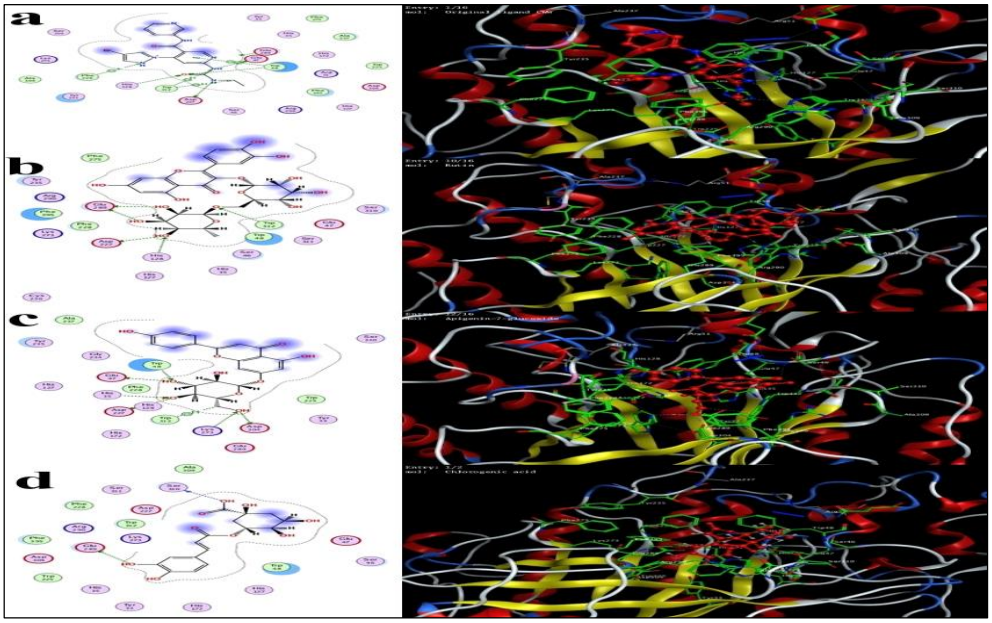

Figure 24. Selected 2D and 3D illustrations of the projected interaction modes and mechanisms of binding between the studied compounds and the alpha-L-fucosidase enzyme active site.
*(**a**) Original ligand NAG, (**b**) Rutin, (**c**) Apeginin-7-glucoside, (**d**) clorogenic acid.*

4. DISCUSSION

4.1. Characterization of chemically synthesized ZnO-NPs

The UV-visible absorption spectrum was primarily employed to analyze the optical characteristics of nanoparticles (Rasha et al., 2021). This optical property aligns with the optical activity of ZnO-NPs that were synthesized using a solvothermal technique (Zak et al., 2011c). The shape, size, and elemental distribution of the obtained chemically synthesized ZnO-NPs were characterized using the STEM, TEM, EDAX, and DLS techniques. Using Fourier transform infrared spectroscopy, the sample showed six functional groups detected at 3150, 1631.48, 1425.14, 1078.98, 447.404, and 370.23 cm^{-1}. The intense and wide peak observed at 3150 cm^{-1} in the upper region was a result of the stretching vibration of hydroxyl (OH) groups (Jayarambabu, 2014; Zafar et al., 2021). FTIR analysis was conducted to determine the potential biomolecules accountable for the bioreduction of zinc oxide nanoparticles. The prior results are consistent with the findings reported in other papers (Mahalakshmi and Vijaya, 2020; Yedurkar et al., 2016; Zak et al., 2011a, 2011c, 2011b).

The XRD is a rapid test providing information on crystal size and structure (Modena et al., 2019). The XRD analysis confirmed that the diffraction peak planes of the precipitated ZnO-NPs were matched well with the quartzite ZnO reported in the joint committee on powder diffraction standards (JCPDS) data (Salih et al., 2021). The measured zeta potential was determined to be −30.214 mV. The zeta potential is directly related to the stability of the nanoparticles while they are in a solution. The nanoparticles produced in this work were highly stable, as evidenced by a zeta potential value of −30.214 mV (Jain et al., 2020).

4.2. Determination of some biochemical and stress markers in the leaves from different treatments of tomato and maize

In tomato, the increase in H_2O_2 (a reactive oxygen substance that increases due to stress and is highly destructive), MDA (a cytotoxin produced by the breakdown of lipid cell membranes due to ROS), proline (an amino acid that increases in reaction to stress and functions as an effective osmolyte), and total hydrolyzable sugar contents in tomato and maize were quite evident under salt stress (Anjum et al., 2022; Hasanuzzaman et al., 2020; Hayat et al., 2012) (Tables 4 and 5). The reason for the increase in MDA and H_2O_2 in plants under salt stress is due to the increase of reactive oxygen species (ROS) and cell membrane damage with stress (Ahmed et al., 2024b). In a separate study on tomatoes, Li (2009) discovered that the salinity caused an increase in the levels of proline and MDA in tomato seedlings . Furthermore, the amount of NaCl had an impact on the soluble sugar content, as Shaba.Zahra et al. (2010) discovered that the levels of soluble sugars and proline in tomatoes rise in

response to increased salt. The study conducted by Faizan et al. (2021) found that tomato seedlings grown in soil containing NaCl showed a reduction in protein content. The decrease in cellular integrity and excessive formation of reactive oxygen species (ROS) was caused by the presence of NaCl (Tavallali et al., 2010).

The H_2O_2, MDA, proline, total free amino acids, and total hydrolyzable sugar levels significantly increased in response of **maize plants** to salt stress (Ahmed et al., 2024a; Anjum et al., 2022) (Table 5). The current study demonstrated that applying zinc oxide nanoparticles to the leaves enhanced the plants' sensitivity to NaCl stress. The preceding report can be attributed to the fact that ZnO nanoparticles enhanced plant resilience to sodium chloride stress by mitigating the generation of ROS and oxidative harm, leading to mitigating the harmful effects of salinization. The decrease in ROS generation is linked to a decline in enzymatic and non-enzymatic antioxidant activity (Mahawar et al., 2024; Rai-Kalal and Jajoo, 2021). Another possible explanation is the impact of ZnO-NPs on the absorption of nutrients, which counteracts the deficit of micro and macronutrients caused by NaCl in plants (Tavanti et al., 2021). In some other studies and in line with the obtained results in the current experiment, evidence has demonstrated that zinc oxide NPs have increased the absorption of calcium, potassium, zinc, iron, and copper in faba bean (Mogazy and Hanafy, 2022) and rapeseed (El-Badri et al., 2021) when exposed to high salinity levels, these components replaced the Na ions, reducing the harmful consequences of Na^+ toxicity.

4.3. Assessment of the antioxidant enzymes from tomato and maize

In plants, ROSs are neutralized by antioxidative enzymes, including superoxide dismutase (SOD), glutathione reductase/-s-transferase (GR/GST), peroxidase (POX), or catalase (CAT) (Mishra et al., 2023). Nonetheless, the presence of NaCl has markedly decreased the activity of antioxidative enzymes in our current study. Nevertheless, a significant finding from this study is that the foliar application of chemically synthesized ZnO-NPs enhanced the activity of antioxidative enzymes, regardless of the presence or absence of NaCl.

Superoxide dismutase facilitates the dismutation of superoxide free radicals into hydrogen peroxide (H_2O_2) and oxygen (O_2), serving as the first defense against oxygen free radicals in the cytosol, chloroplast, and mitochondria (Demidchik, 2015; El-Zohri et al., 2021). Catalase (CAT) and other peroxidases serve as significant scavengers of $O_2^{\bullet-}$ free radicals in the produced H_2O_2 from SOD, which are transformed into H_2O and O_2 (Smirnoff, 1998). CAT can effectively decompose elevated levels of hydrogen peroxide (H_2O_2) and mitigate the harm caused by hydroxyl radicals ($OH^{\bullet}$) generated by H_2O_2. Faizan et al. (2021) studied the activity of antioxidant enzymes, including SOD, POX, and CAT. They found that those enzymes exhibited an

upward trend in plants treated with ZnO-NPs and NaCl relative to the control group. The highest enhancement in the activity of CAT (57%), SOD (44%), and POX (59%) was observed in plants treated with 50 mg/L of ZnO-NPs in conjunction with NaCl (Faizan et al., 2021b).

Glutathione reductase (GR), or glutathione disulfide reductase (GSR), is a flavoprotein classified under the NADPH-dependent oxidoreductase family. It facilitates the conversion of oxidized glutathione (glutathione disulfide) (GSSG) to reduced glutathione (GSH), which is crucial for cellular defense against reactive oxygen species (ROS) (Vokkaliga et al., 2017). GSTs exhibiting GSH-dependent reductase activity, such as dehydroascorbate reductase (DHAR) and glutathione-s-transferase lambda class GSTL, may contribute to the preservation of reductants pools (including ascorbic acid, α-tocopherol, and anthocyanins), while other isoenzymes facilitate the detoxification of reactive metabolites (Csiszár et al., 2014; Dixon and Edwards, 2010). The GST activity depletes GSH, which explains why the overproduction of GST competes with other antioxidant mechanisms. In tomatoes, salt reduces ascorbic acid and glutathione (GSH) levels and promotes lipid peroxidation (Mittova et al., 2004). Maintaining a high ratio of GSH/GSSG is crucial for the salt and drought tolerance of tomato, maize, and wheat (Csiszár et al., 2014; Shalata and Neumann, 2001). The previous results were in line with the current study's results.

Recent research has revealed the significance of nanotechnology in enhancing the ability of many plant species to tolerate salt. The primary aim of this work was to clarify the function of ZnO nanoparticles in the modulation of salt (NaCl) stress tolerance in tomato plants, and how the salt stress and foliar application may contribute to changes on the transcriptomic level. Plants exposed to NaCl stress accumulate ROS; nonetheless, maintaining an equilibrium between the generation and degradation of ROS is crucial to prevent oxidative damage (Mohammad Faizan et al., 2021; Meneguzzo et al., 1999). El-Zohri et al. (2021) proved that, in response to green ZnO-NPs foliar application, antioxidant enzymes such as SOD, CAT, and APX were increased in tomato plants to reduce the negative effects of drought stress by reducing oxidative stress.

4.4. Transcriptomic analysis of the extracted RNA from tomato and maize

The study aimed to reproduce the workflow using transcriptome analysis using the OmicsBox tool, specifically the functional analysis and transcriptomics modules. This involved obtaining sequencing data and performing a combined differential expression analysis of the whole transcriptome (supertranscript) within OmicsBox. This provided a solid foundation for further analysis and ensuring comparability with up- and down-regulated sequences.

The top 50 up- and down-regulated sequences were examined to visualize gene expression across samples and their associated biochemical pathways. For ***Solanum lycopersicum* L.**, there were 112 sequences linked to different pathways, such as arsenic uptake and detoxification, cytosolic glycolysis, TCA cycle (plant), Calvin cycle, sucrose biosynthesis, regulation of seed germination and coleoptile growth under submergence and normal gravity environment, choline biosynthesis I, and short day regulated expression of florigens.

For comparison between T1 and T2, there were 102 sequences linked to different pathways in the plant reactome database, including photorespiration, cytosolic glycolysis, starch biosynthesis, and sucrose biosynthesis. There were 221 linked down-regulated sequences, including 16 genes for sterol biosynthesis, 9 for seed germination and coleoptile growth under submergence and normal gravity environment, 7 for mevalonate pathway, 5 for leucodelphinidin biosynthesis, and 9 for galactosylcyclitol biosynthesis. For comparison between T1 and T5, there were 76 sequences linked to different pathways, 471 down-regulated sequences, and 176 sequences linked to different pathways. Comparing T4 with T5 revealed 26 sequences linked to different pathways, 44 down-regulated sequences, and 61 down-regulated sequences.

Salinity stress significantly elevated the expression of genes involved in the metabolism of purine, thiamine, starch, sucrose, and other secondary metabolites in plants (Decsi et al., 2025). Salt stress increases and prolongs starch buildup in early fruit development (Yin et al., 2010). In the studies by Balibrea et al. (1999) (1996), it was found that salt stress had negatively affected starch accumulation, and this occurred due to the complete breakdown of transiently generated starch into soluble sugars in mature tomato fruits. Yin et al. (2010) found that the increase of starch accumulation may increase sugar content in salt-stressed red tomato fruits. Balibrea et al. (2006) discovered that sucrose import during ripening enhanced sugar concentration in wild species under saline stress, suggesting various germplasm processes regulate sugar levels. Sun et al. (2020a) discovered that foliar application of ZnO nanoparticles increased zinc in leaves while decreasing zinc in roots. The findings indicated that the increased Zn^{2+} in leaves negatively regulates Zn^{2+} transport to the roots.

Li et al. (2025) proved that the primary trend in the gene expression profile associated with metabolic pathways, secondary metabolite biosynthesis, plant hormone signal transduction, and carbon metabolism was enhanced following drought treatment in rice. Conversely, the down-regulated differentially expressed genes (DEGs) were predominantly associated with metabolic pathways and the manufacture of secondary metabolites. The findings of the current study revealed that under salinity stress, tomato leaves

can respond to environmental changes by modulating the expression of genes associated with specific adaptive biological processes. Notably, analysis of the DEGs revealed that several genes associated with purine metabolism exhibited responsiveness to salinity and ZnO-NPs, suggesting that this pathway is crucial for the adaptive response to salinity stress in tomato.

***Zea mays* L.**, a plant species, has been compared in the plant reactome database between M1 and M2, with 21 sequences linked to different pathways. These pathways include abscisic acid mediated signalling, HSFA7/HSFA6B-regulatory network-induced by drought and ABA, polyisoprenoid biosynthesis, TCA cycle (plant), and mevalonate pathway. Additionally, there are 303 down-regulated linked sequences (genes) in the same database. For comparisons between M1 and M3, there are 50 sequences linked to different pathways, including sucrose biosynthesis, sulfate activation for sulfonation, starch biosynthesis, and cyanate degradation. 130 linked down-regulated sequences (genes) are also present.

For comparisons between T1 and T3, there are 28 sequences linked to different pathways, including myo-inositol biosynthesis, polyisoprenoid biosynthesis, Calvin cycle, polar auxin transport, and trehalose biosynthesis I. 207 down-regulated sequences (genes) are also present. For comparisons between M2 and M3, *Zea mays* L. shows 105 sequences linked to different pathways, including polyisoprenoid biosynthesis, valine degradation, glutathione redox reactions II, nitrate assimilation, and vitamin E biosynthesis. Additionally, there are 5 down-regulated linked sequences (genes) in the same database.

Salinity stress dramatically increased transcript abundance of thiamine biosynthesis genes (THI4, THIC, TH1, and TPK). The transcript expressions are highest in leaves, supporting the assumption that thiamine production occurs in chloroplasts (Yusof, 2019). Increasing polyethylene glycol (PEG) and NaCl concentrations caused osmotic and salt stress, leading to a substantial rise in total thiamine content in maize seedlings. In maize seedlings, higher thiamine levels were linked to higher abscisic acid (ABA) levels (Tunc-Ozdemir et al., 2009). Additionally, drought and salinity stress conditions led to a slight increase in transketolase activity, a key TPP-dependent enzyme. The disruption of transketolase activity shows that thiamine metabolism plays a role in plant stress adaptation (Tunc-Ozdemir et al., 2009).

4.5. Antimicrobial activities of tomato and maize extracts

Tomato and maize plants subjected to salt stress may exhibit altered leaf extract compositions, potentially affecting their efficacy in combating pathogens. Certain studies indicated that salt stress can induce leaves to synthesize increased levels of chemicals, including antioxidants and phenolic compounds. This may enhance the leaves' efficacy in combating pathogens.

Conversely, additional studies indicated that salt stress might adversely affect certain plant traits, thereby diminishing their capacity to combat pathogens.

The increased antibacterial efficacy of extracts from ZnO-treated plants is apparent, although the possible influence of residual zinc should be acknowledged. Zinc ions are recognized for their bioaccumulation in leaf tissues after foliar application (Rossi et al., 2019). Despite the mitigatory concentrations employed in this work (75 and 150 mg/L), it is conceivable that trace quantities of Zn^{2+} were sequestered in the extracts. The observed antibacterial activity should be viewed as a synergistic effect: a confluence of nanoparticle-induced metabolic flux (elevated phenolics and flavonoids) and the presence of trace bioactive zinc.

The significant enhancement in antibacterial activity following the application of ZnO-NPs cannot be attributed to a single factor. Our observations indicated a significant increase in phenolic and flavonoid concentrations; nevertheless, it is essential to recognize that bioaccumulated Zn^{2+} or nanoparticles absorbed by cells may be responsible for this phenomenon. Zinc is an acknowledged antibacterial agent; however, its role in our extracts likely functions as a potentiator rather than the sole active ingredient. We propose a synergistic mechanism wherein ZnO-induced metabolites (e.g., quercetin, gallic acid) undermine the structural integrity of the bacterial cell wall, hence increasing the pathogen's susceptibility to trace Zn^{2+} ions. The results should be interpreted as an enhanced plant-defense response that produces a more potent biocomposite extract.

4.6. Analysis of docking results

Molecular docking commonly used to discover the optimal orientation of a ligand (a single compound or a group) to a target receptor as well as to thoroughly examine the mode of interaction and binding energy for this ligand/s (Mostafa et al., 2025). In this investigation, docking was employed as a reliable and effective method to evaluate the antibacterial activity of tomato and maize leaves extracts *in silico* and validate the *in vitro* findings. Additionally, to comprehend how the molecules they contain will interact with DNA Gyrase (PDB Id: 3TTZ), CYP51 (PDB Id: 5FSA), DNA Gyrase (PDB ID: 6F86), and alpha−L−fucosidase enzyme (PDB Id: 9LXL), four possible antimicrobial targets. According to HPLC analysis, tomato and maize leaves included 17 polyphenols and flavonoids, which are naturally occurring substances that may be found in a variety of plant sources and have demonstrated promising antimicrobial action.

Phenolic compounds may have an antibacterial effect because they can permeabilize and destabilise the cytoplasmic membrane, block essential enzymes, and affect DNA synthesis (Borges et al., 2013). DNA Gyrase enzyme is a necessary component of bacterial cells and plays important roles

in transcription, replication, and repair processes, all of which are critical to cell life and reproduction (Andrade-Pavón et al., 2024). Lanosterol 14α-demethylase (CYP51), an enzyme essential for preserving the integrity of fungal cell membranes, is inhibited by conventional antifungal drugs like azoles, which target ergosterol production (Zhang et al., 2024).

Despite the identified metabolites demonstrating significant binding affinities for target proteins, these *in silico* predictions should not be considered conclusive evidence of biological activity. Crude plant extracts are complex mixtures; hence, the antimicrobial capabilities found may be affected by synergistic or antagonistic interactions that cannot only be clarified via the docking of an individual molecule. Furthermore, this data provides a theoretical basis for the proposed mechanism of action. Further study employing bio-guided separation and purification of these metabolites is essential to validate these computational predictions.

5. CONCLUSIONS AND RECOMMENDATIONS

Saline impacts arise from intricate interactions among morphological, physiological, and biochemical processes, encompassing seed germination, plant growth, and the uptake of water and nutrients. Plant growth is negatively affected by early salt stress. This ultimately decreases crop output in saline environments, affecting both the quality and quantity of plant products. This underscores the necessity of researching procedures for using manufactured nanoparticles to regulate plants' physiological responses to adverse environments.

In case of tomato plants, dosages of ZnO-NPs had a significant effect across treatments. ZnO-NPs also increased chlorophyll, reduced stress markers, and released phenolic chemicals and proteins in the leaves of tomatoes. ZnO-NPs reduce salt stress by promoting the uptake of minerals. ZnO-NPs had beneficial effects on tomato plants under salt stress, making them an alternative approach to enhance resilience in saline soils or low-quality irrigation water. This study examined how foliar application of chemically synthesized ZnO-NPs to the leaves affected biochemistry, morphology, and phenolic compound synthesis with and without NaCl. It would be beneficial to conduct further research on the impacts at the enzyme and molecular levels to obtain more comprehensive and precise findings. Furthermore, to further the investigation, it is possible to undertake studies that extend to fruit yield and ripening in plants to optimize the dosages of zinc oxide nanoparticles applied via foliar spray in an open-field experiment.

All treatments showed significant changes in maize plant growth and development after applying zinc oxide NPs. ZnO-NPs increased chlorophyll and lowered stress. ZnO-NPs enhanced the ability of maize plants to withstand the adverse conditions of saline soils or low-quality irrigation water. This field study investigated the effect of zinc oxide nanoparticles on maize plant leaves when saline water is used for irrigation during the growing season. This study also examined how this foliar treatment affected plant biochemistry, morphology, fatty acid synthesis, and crop production when NaCl is present and when it is not. Considering the characteristics of ZnO-NPs in maize plants under salt stress, it might be considered a feasible option for cultivating areas with restricted availability of high-quality irrigation water.

While the obtained results demonstrated the high potential of ZnO-NPs, it is important to note that the efficacy of the different treatments and their influences on tomato and maize crops may vary depending on soil type, environmental humidity, genotype of the crop under investigation, dosage of the salinity stressor, dosage of the sprayed nanoparticles, and the area of the experiment weather it is under the greenhouse or in the open field, etc.

6. NOVEL SCIENTIFIC RESULTS

1. Understanding the potential benefits of using ZnO-NPs in *Solanum lycopersicum* L. and *Zea mays* L. cultivation ultimately contributes to sustainable agriculture and a secure food supply.
2. Exogenous foliar application of 75 & 150 mg/L and 2 g/L ZnO-NPs on *Solanum lycopersicum* L. and *Zea mays* L. is associated with measurable changes in chlorophyll-related traits, oxidative stress markers, phenolic compounds, fatty acids, and nutrient-related physiological parameters in the studied plants under salinity stress (150 mM NaCl).
3. Foliar treatment with 75 and 150 mg/L ZnO-NPs in *Solanum lycopersicum* L. provided a biochemical shield against 150 mM NaCl stress by counteracting salinity-induced inhibition of SOD, CAT, and GR enzymes. This treatment creates a better antioxidant balance by increasing the levels of POX and GST, which act together. This blocked ROS from damaging membranes and maintained photosynthesis.
4. The application of ZnO-NPs (2 g/L) in *Zea mays* L. established an optimal antioxidant equilibrium during stress induced by 150 mM NaCl. This is characterized by the reactivation of inhibited SOD, CAT, and GR activities, alongside a strategic reduction in the excessive activation of POX and GST (by 55–61%). This improved enzyme profile reduces the metabolic contribution to defense, hence decreasing lipid peroxidation and maintaining cellular health in saline conditions.
5. Foliar application of ZnO-NPs (75 and 150 mg/L) alleviated salinity stress (150 mM) in *Solanum lycopersicum* L. by activating a comprehensive transcriptome reconfiguration. This molecular priming effect was characterized by the upregulation of pathways for carbon and nitrogen assimilation and the activation of gene clusters for secondary metabolism. This triggered the antioxidant enzymatic defense system (such as SOD, CAT, and GST), which, at 150 mM NaCl salinity, would have otherwise slowed.
6. In *Zea mays* L., foliar ZnO-NP treatment (2 g/L) alleviated 150 mM NaCl stress by reversing the extensive transcriptional suppression of more than 8,000 genes. The nanoparticles stabilized metabolism by increasing the activity of pathways that generate energy (oxidative phosphorylation) and nitrogen (arginine/proline), while also improving maize's ability to respond to oxidative stress, thereby stimulating ROS-detoxifying pathways.
7. Under 150 mM NaCl stress, the application of 75 and 150 mg/L ZnO-NPs to the leaves of *Solanum lycopersicum* L. enhanced the efficacy of leaf extracts against bacterial and fungal pathogens such as *E. coli*, *Staph. aureus*, and *Aspergillus niger*, etc. The augmented synthesis of bioactive

compounds like Rutin and Apeginin-7-glucoside, confirmed by molecular docking to exhibit substantial binding affinities (up to −7.0 kcal/mol) to pathogen target proteins (Topoisomerase II ATPase enzyme) (DNA Gyrase) (PDB Id: 3TTZ) and sterol 14-alpha demethylase (CYP51) (PDB Id: 5FSA), respectively.

8. In *Zea mays* L., under 150 mM NaCl stress, the application of 2 g/L ZnO-NPs to leaves enhanced the efficacy of leaf extracts against bacterial and fungal pathogens, including *B. cereus*, *S. typhi*, *A. flavus*, and *P. vercosum*, etc. The molecular docking analysis confirmed that the augmented synthesis of bioactive compounds, such as Rutin, exhibited significant binding affinities (up to −7.0 kcal/mol) to both pathogen target proteins (Topoisomerase II ATPase enzyme) (DNA Gyrase) (PDB Id: 6F86), and the alpha-L-fucosidase (PDB Id: 9LXL). This demonstrated a novel link between ZnONPs-mediated salt tolerance and enhanced biotic defense.

7. LIST OF PUBLICATIONS AND CONFERENCES

7.1. PUBLICATIONS

PUBLICATIONS RELATED TO PHD STUDIES

Ahmed, M.; Decsi, K.; Tóth, Z. Different Tactics of Synthesized Zinc Oxide Nanoparticles, Homeostasis Ions, and Phytohormones as Regulators and Adaptatively Parameters to Alleviate the Adverse Effects of Salinity Stress on Plants. Life 2023, 13, 73. https://doi.org/10.3390/life13010073

Ahmed, M.*; Tóth, Z.; Decsi, K. The Impact of Salinity on Crop Yields and the Confrontational Behavior of Transcriptional Regulators, Nanoparticles, and Antioxidant Defensive Mechanisms under Stressful Conditions: A Review. Int. J. Mol. Sci. 2024, 25, 2654. https://doi.org/10.3390/ijms25052654

Ahmed, M.; Marrez, D.A.; Rizk, R.; Zedan, M.; Abdul-Hamid, D.; Decsi, K.; Kovács, G.P.; Tóth, Z. The Influence of Zinc Oxide Nanoparticles and Salt Stress on the Morphological and Some Biochemical Characteristics of *Solanum lycopersicum* L. Plants. Plants 2024, 13, 1418. https://doi.org/10.3390/plants13101418

Ahmed, M.; Marrez, D.A.; Rizk, R.; Abdul-Hamid, D.; Tóth, Z.; Decsi, K. Interventional Effect of Zinc Oxide Nanoparticles with *Zea mays* L. Plants When Compensating Irrigation Using Saline Water. Nanomaterials 2024, 14, 1341. https://doi.org/10.3390/nano14161341

Ahmed, M.*, Tóth, Z., Marrez, D.A., Rizk, R., Abdul-Hamid, D., Decsi, K., **2025**. Transcriptome datasets of salt-stressed tomato plants treated

with zinc oxide nanoparticles. Data in Brief 58, 111282. https://doi.org/10.1016/j.dib.2025.111282

Ahmed, M.*; Tóth, Z.; Rizk, R.; Abdul-Hamid, D.; Decsi, K. Investigation of Antioxidative Enzymes and Transcriptomic Analysis in Response to Foliar Application of Zinc Oxide Nanoparticles and Salinity Stress in *Solanum lycopersicum*. *Agronomy* **2025**, *15*, 1715. https://doi.org/10.3390/agronomy15071715

Ahmed, M.; Tóth, Z.; Rizk, R.; Nasir, M.W.; Decsi, K. Ecofriendly Application of Synthetic Zinc Oxide Nanoparticles as Stress Regulator Bio-Fertilizer for *Zea mays*. Agronomy 2025, 15, 2875. https://doi.org/10.3390/agronomy15122875

Ahmed, M.; Abd-El Fatah, S.I.; Shaker, A.S.; Tóth, Z.; Decsi, K. The Role of Zinc Oxide Nanoparticles in Boosting Tomato Leaf Quality and Antimicrobial Potency. *Oxygen* **2026**, *6*, 2. https://doi.org/10.3390/oxygen6010002

PUBLICATIONS RELATED TO OTHER PROJECTS

Ahmed, M.; Marrez, D.A.; Abdelmoeen, N.M.; Mahmoud, E.A.; Abdel-Shakur Ali, M.; Decsi, K.; Tóth, Z. Proximate Analysis of *Moringa oleifera* Leaves and the Antimicrobial Activities of Successive Leaf Ethanolic and Aqueous Extracts Compared with Green Chemically Synthesized Ag-NPs and Crude Aqueous Extract against Some Pathogens. Int. J. Mol. Sci. 2023, 24, 3529. https://doi.org/10.3390/ijms24043529

Ahmed, M.; Marrez, D.A.; Mohamed Abdelmoeen, N.; Abdelmoneem Mahmoud, E.; Ali, M.A.-S.; Decsi, K.; Tóth, Z. Studying the Antioxidant and the Antimicrobial Activities of Leaf Successive Extracts Compared to the Green-Chemically Synthesized Silver Nanoparticles and the Crude Aqueous Extract from *Azadirachta indica*. Processes 2023, 11, 1644. https://doi.org/10.3390/pr11061644

Decsi, K.; **Ahmed, M.**; Rizk, R.; Abdul-Hamid, D.; Kovács, G.P.; Tóth, Z. Emerging Trends in Non-Protein Amino Acids as Potential Priming Agents: Implications for Stress Management Strategies and Unveiling Their Regulatory Functions. Int. J. Mol. Sci. 2024, 25, 6203. https://doi.org/10.3390/ijms25116203

Decsi, K.; **Ahmed, M.***; Rizk, R.; Abdul-Hamid, D.; Vaszily, Z.; Tóth, Z. Transcriptome Datasets of Maize Plant Cultures Treated with Humic- and Amino Acids. Data in Brief 2024, 57, 110900. https://doi.org/10.1016/j.dib.2024.110900

Decsi, K.; **Ahmed, M.***; Rizk, R.; Abdul-Hamid, D.; Tóth, Z. Analysis of Plant Physiological Parameters and Gene Transcriptional Changes Under the Influence of Humic Acid and Humic Acid-Amino Acid

Combinations in Maize. Int. J. Mol. Sci. **2024**, *25*, 13280. https://doi.org/10.3390/ijms252413280

Rizk, R.; **Ahmed, M.***; Abdul-Hamid, D.; Zedan, M.; Tóth, Z.; Decsi, K. Resulting Key Physiological Changes in *Triticum aestivum* L. Plants Under Drought Conditions After Priming the Seeds with Conventional Fertilizer and Greenly Synthesized Zinc Oxide Nanoparticles from Corn Wastes. Agronomy 2025, 15, 211. https://doi.org/10.3390/agronomy15010211

Decsi, K.; **Ahmed, M.***; Abdul-Hamid, D.; Tóth, Z. The Role of Salicylic Acid in Activating Plant Stress Responses—Results of the Past Decade and Future Perspectives. Int. J. Mol. Sci. 2025, 26, 4447. https://doi.org/10.3390/ijms26094447

Decsi, K.; **Ahmed, M.***; Abdul-Hamid, D.; Rizk, R.; Tóth, Z. Verification of Seed-Priming-Induced Stress Memory by Genome-Wide Transcriptomic Analysis in Wheat (*Triticum aestivum* L.). *Agronomy* **2025**, *15*, 1365. https://doi.org/10.3390/agronomy15061365

Decsi, K., **Ahmed, M.***, Vaszily, Z., Abdul-Hamid, D., Tóth, Z., **2025**. Transcriptomic analysis of the combined effects of humic acids and nutrients in maize (*Zea mays* L.) (In Hungarian language). Növénytermelés. 74(3): 5-30.

Decsi, K., **Ahmed, M.***, Rizk, R., Abdul-Hamid, D., Tóth, Z., **2025**. Transcriptome datasets of wheat plant cultures treated with seed priming fertilizer. Data Brief 62, 112050. https://doi.org/10.1016/j.dib.2025.112050

Decsi, K.; **Ahmed, M.***; Tóth, Z. Genome-Wide Transcriptional Analysis Reveals Gamma-Aminobutyric Acid (GABA) Priming Induces Long-Term Stress Memory in Tomato (*Solanum lycopersicum*). Agriculture 2025, 15, 2012. https://doi.org/10.3390/agriculture15192012

Muhammad, A.-R.H.; Marrez, D.A.; **Ahmed, M.***; Shaker, A.S.; Mohamed, R.S.; Barakat, O.S. Biotransformation of Microalgal Biomass by Lactic Acid Bacteria and *Saccharomyces cerevisiae*: Implications for Food and Sustainability. Oxygen 2025, 5, 23. https://doi.org/10.3390/oxygen5040023

7.2. CONFERENCES

Georgikon days, Georgikon campus, MATE University, Keszthely–Hungary. Polyphenolic attributes of *Moringa oleifera* leaf ethanolic and aqueous extracts and the protective contribution of its green-chemically synthesized Ag-NPs against food-borne pathogenic bacteria and crop-infecting fungi. Authors: Mostafa Ahmed, Zoltán Tóth, and Kincső Decsi. Date: 17-18, November, 2022

The 13th ICEEE-2022 Online, International Annual Conference on "Global Environmental Development & Sustainability: Research, Engineering & Management", Óbuda University, Budapest – Hungary. Antioxidant activity of *Azadirachta indica* leaf successive extracts and the susceptibility of different pathogenic bacteria and mycotoxigenic fungi to its green-chemically synthesized silver nanoparticles and various extracts. Authors: Mostafa Ahmed, Diaa Attia, Nadia Mohamed, Ebtesam Abdelmoneem, Mohamed Abdel-Shakur, Kincső Decsi and Zoltán Tóth. Date: 17-18, November, 2022

KAN University days conference, MATE University, Kaposvár campus, Kaposvár-Hungary. Harmful effects of NaCl stress on photosynthetic & growth attributes, and nutrient distribution on the leaves of tomato Kecskeméti-549 and how the chemically synthesized zinc oxide nanoparticles can mitigate and compensate the stress conditions. Authors: Mostafa Ahmed, Kincső Decsi, Zoltán Tóth. Date: 28-9-2023

XXXV. Keszthely Plant Protection Forum, Georgikon campus, Keszthely, Hungary. Investigation of the harmful effects of xenobiotic-induced stress and the possibilities of their elimination with plant conditioning preparations in sunflower stands. Authors: Imre Gréta Anna, Both Gyula, Mostafa Ahmed, Decsi Kincső. Date: January 14-16, 2026.

8. REFERENCES

Abbasi, G.H., Akhtar, J., Ahmad, R., Jamil, M., Anwar-Ul-Haq, M., Ali, S., Ijaz, M., 2015. Potassium application mitigates salt stress differentially at different growth stages in tolerant and sensitive maize hybrids. Plant Growth Regul 76, 111–125.

Ahanger, M.A., Agarwal, R.M., Tomar, N.S., Shrivastava, M., 2015. Potassium induces positive changes in nitrogen metabolism and antioxidant system of oat (Avena sativa L. cultivar Kent. J. Plant Interact 10, 211–223.

Ahmed, M., Marrez, D.A., Abdelmoeen, N.M., Mahmoud, E.A., Abdel-Shakur Ali, M., Decsi, K., Tóth, Z., 2023a. Proximate Analysis of Moringa oleifera Leaves and the Antimicrobial Activities of Successive Leaf Ethanolic and Aqueous Extracts Compared with Green Chemically Synthesized Ag-NPs and Crude Aqueous Extract against Some Pathogens. International Journal of Molecular Sciences 24, 3529. https://doi.org/10.3390/ijms24043529

Ahmed, M., Marrez, D.A., Mohamed Abdelmoeen, N., Abdelmoneem Mahmoud, E., Ali, M.A.-S., Decsi, K., Tóth, Z., 2023b. Studying the Antioxidant and the Antimicrobial Activities of Leaf Successive Extracts Compared to the Green-Chemically Synthesized Silver Nanoparticles and the Crude Aqueous Extract from Azadirachta indica. Processes 11, 1644. https://doi.org/10.3390/pr11061644

Ahmed, M., Marrez, D.A., Rizk, R., Zedan, M., Abdul-Hamid, D., Decsi, K., Kovács, G.P., Tóth, Z., 2024a. The Influence of Zinc Oxide Nanoparticles and Salt Stress on the Morphological and Some Biochemical Characteristics of Solanum lycopersicum L. Plants. Plants 13, 1418. https://doi.org/10.3390/plants13101418

Ahmed, M., Tóth, Z., Decsi, K., 2024b. The Impact of Salinity on Crop Yields and the Confrontational Behavior of Transcriptional Regulators, Nanoparticles, and Antioxidant Defensive

Mechanisms under Stressful Conditions: A Review. International Journal of Molecular Sciences 25, 2654. https://doi.org/10.3390/ijms25052654
Ahmed, M., Tóth, Z., Marrez, D.A., Rizk, R., Abdul-Hamid, D., Decsi, K., 2025. Transcriptome datasets of salt-stressed tomato plants treated with zinc oxide nanoparticles. Data in Brief 58, 111282. https://doi.org/10.1016/j.dib.2025.111282
Alexieva, V., Sergiev, I., Mapelli, S., Karanov, E., 2001. The effect of drought and ultraviolet radiation on growth and stress markers in pea and wheat. Plant, Cell & Environment 24, 1337–1344. https://doi.org/10.1046/j.1365-3040.2001.00778.x
Anjum, N., Gill, S., Corpas, F., Ortega Villasante, C., Hernández, L.E., Tuteja, N., Sofo, A., Hasanuzzaman, M., Fujita, M., 2022. Editorial: Recent Insights Into the Double Role of Hydrogen Peroxide in Plants. Frontiers in Plant Science 13, 843274. https://doi.org/10.3389/fpls.2022.843274
Anjum, N.A., Gill, S.S., Corpas, F.J., Ortega-Villasante, C., Hernandez, L.E., Tuteja, N., Sofo, A., Hasanuzzaman, M., Fujita, M., 2022. Editorial: Recent Insights Into the Double Role of Hydrogen Peroxide in Plants. Front. Plant Sci. 13. https://doi.org/10.3389/fpls.2022.843274
A.T.C.C., 1984. American Type Culture Collection, 13th ed. USA.
Balibrea, M., Parra, M., Bolarín, M., Pérez-Alfocea, F., 1999. Cytoplasmic sucrolytic activity controls tomato fruit growth under salinity. Australian Journal of Plant Physiology 26, 561–568.
Balibrea, M., Santa Cruz, A., Bolarín, M., Pérez-Alfocea, F., 1996. Sucrolytic activities in relation to sink strength and carbohydrate composition in tomato fruit growing under salinity. Plant Science 118, 47–55.
Balibrea, M.E., Martínez-Andújar, C., Cuartero, J., Bolarín, M.C., Pérez-Alfocea, F., 2006. The high fruit soluble sugar content in wild Lycopersicon species and their hybrids with cultivars depends on sucrose import during ripening rather than on sucrose metabolism. Funct Plant Biol 33, 279–288. https://doi.org/10.1071/FP05134
Bates, L.S., Waldren, R.P., Teare, I.D., 1973. Rapid determination of free proline for water-stress studies. Plant and Soil. https://doi.org/10.1007/BF00018060
Bauer, A., Kirby, W., Sheriss, J., Turck, M., 1996. Antibiotic susceptibility testing by standardized single method. Am. J. Clin. Pathol 45, 493–496.
Beauchamp, C., Fridovich, I., 1971. Superoxide dismutase: Improved assays and an assay applicable to acrylamide gels. Analytical Biochemistry 44, 276–287. https://doi.org/10.1016/0003-2697(71)90370-8
Berkhout, S.W., Haaf, J.M., Gronau, Q.F., Heck, D.W., Wagenmakers, E.-J., 2024. A tutorial on Bayesian model-averaged meta-analysis in JASP. Behav Res 56, 1260–1282. https://doi.org/10.3758/s13428-023-02093-6
Bonnichsen, R.K., Chance, B., Theorell, H., 1947. Catalase Activity. Acta Chem. Scand 1, 685–709. https://doi.org/10.1016/j.abb.2012.01.015
Bradford, M.M., 1976. A rapid and sensitive method for the quantitation of microgram quantities of protein utilizing the principle of protein-dye binding. Analytical Biochemistry. https://doi.org/10.1016/0003-2697(76)90527-3
Chabi, I.B., Zannou, O., Dedehou, E.S.C.A., Ayegnon, B.P., Oscar Odouaro, O.B., Maqsood, S., Galanakis, C.M., Pierre Polycarpe Kayodé, A., 2024. Tomato pomace as a source of valuable functional ingredients for improving physicochemical and sensory properties and extending the shelf life of foods: A review. Heliyon 10, e25261. https://doi.org/10.1016/j.heliyon.2024.e25261
Chance, B., Maehly, A.C., 1955. [136] Assay of catalases and peroxidases:, in: Methods in Enzymology. Academic Press, pp. 764–775. https://doi.org/10.1016/S0076-6879(55)02300-8
Chaudhary, D., Kumar, A., Kumar, R., Singode, A., Mukri, G., Sah, R., Tiwana, U., Kumar, B., 2016. Evaluation of normal and specialty corn for fodder yield and quality traits. Range Management and Agroforestry 37, 79–83.
Csiszár, J., Horváth, E., Váry, Z., Gallé, Á., Bela, K., Brunner, S., Tari, I., 2014. Glutathione transferase supergene family in tomato: Salt stress-regulated expression of representative genes from distinct GST classes in plants primed with salicylic acid. Plant Physiology and Biochemistry 78, 15–26. https://doi.org/10.1016/j.plaphy.2014.02.010
Cuajungco, M.P., Ramirez, M.S., Tolmasky, M.E., 2021. Zinc: Multidimensional Effects on Living Organisms. Biomedicines 9, 208. https://doi.org/10.3390/biomedicines9020208

Decsi, K., Ahmed, M., Abdul-Hamid, D., Rizk, R., Tóth, Z., 2025. Verification of Seed-Priming-Induced Stress Memory by Genome-Wide Transcriptomic Analysis in Wheat (Triticum aestivum L.). Agronomy 15, 1365. https://doi.org/10.3390/agronomy15061365

Demidchik, V., 2015. Mechanisms of oxidative stress in plants: From classical chemistry to cell biology. Environmental and Experimental Botany 109, 212–228. https://doi.org/10.1016/j.envexpbot.2014.06.021

Dixon, D.P., Edwards, R., 2010. Glutathione Transferases. arbo.j 2010. https://doi.org/10.1199/tab.0131

El-Badri, A.M., Batool, M., Mohamed, I.A., Khatab, A., Sherif, A., Wang, Z., 2021. Modulation of salinity impact on early seedling stage via nano-priming application of zinc oxide on rapeseed (Brassica napus L. Plant Physiology and Biochemistry 166, 376–392.

El-Zohri, M., Al-Wadaani, N.A., Bafeel, S.O., 2021. Foliar Sprayed Green Zinc Oxide Nanoparticles Mitigate Drought-Induced Oxidative Stress in Tomato. Plants 10, 2400. https://doi.org/10.3390/plants10112400

Faizan, M., Bhat, J.A., Chen, C., Alyemeni, M.N., Wijaya, L., Ahmad, P., Yu, F., 2021. Zinc oxide nanoparticles (ZnO-NPs) induce salt tolerance by improving the antioxidant system and photosynthetic machinery in tomato. Plant Physiology and Biochemistry 161, 122–130. https://doi.org/10.1016/j.plaphy.2021.02.002

Faizan, Mohammad, Bhat, J.A., Chen, C., Alyemeni, M.N., Wijaya, L., Ahmad, P., Yu, F., 2021. Zinc oxide nanoparticles (ZnO-NPs) induce salt tolerance by improving the antioxidant system and photosynthetic machinery in tomato. Plant Physiology and Biochemistry 161, 122–130. https://doi.org/10.1016/j.plaphy.2021.02.002

Gaafar, R., Diab, R., Halawa, M., Elshanshory, A., El-Shaer, A., Hamouda, M., 2020. Role of Zinc Oxide Nanoparticles in Ameliorating Salt Tolerance in Soybean. Egyptian Journal of Botany 60, 733–747. https://doi.org/10.21608/ejbo.2020.26415.1475

Gengmao, Z., Shihui, L., Xing, S., Yizhou, W., Zipan, C., 2015. The role of silicon in physiology of the medicinal plant (Lonicera japonica L.) under salt stress. Sci. Rep 5, 12696.

Habig, W.H., Pabst, M.J., Jakoby, W.B., 1974. Glutathione S-transferases: The first enzymatic step in mercapturic acid formation. J. Biol. Chem 249, 7130–7139.

Hasanuzzaman, M., Bhuyan, M.H.M.B., Zulfiqar, F., Raza, A., Mohsin, S.M., Mahmud, J.A., Fujita, M., Fotopoulos, V., 2020. Reactive Oxygen Species and Antioxidant Defense in Plants under Abiotic Stress: Revisiting the Crucial Role of a Universal Defense Regulator. Antioxidants (Basel) 9, 681. https://doi.org/10.3390/antiox9080681

Hayat, S., Hayat, Q., Alyemeni, M.N., Wani, A.S., Pichtel, J., Ahmad, A., 2012. Role of proline under changing environments. Plant Signal Behav 7, 1456–1466. https://doi.org/10.4161/psb.21949

Heath, R.L., Packer, L., 1968. Photoperoxidation in isolated chloroplasts. I. Kinetics and stoichiometry of fatty acid peroxidation. Arch Biochem Biophys 125, 189–198. https://doi.org/10.1016/0003-9861(68)90654-1

Hoffmann, T., Hofman, A., Wagenmakers, E.-J., 2022. Bayesian Tests of Two Proportions: A Tutorial With R and JASP. Methodology 18, 239–277. https://doi.org/10.5964/meth.9263

Imakumbili, M.L.E., Semu, E., Semoka, J.M.R., Abass, A., Mkamilo, G., 2021. Managing cassava growth on nutrient poor soils under different water stress conditions. Heliyon 7, e07331. https://doi.org/https://doi.org/10.1016/j.heliyon.2021.e07331

Inculet, C.-S., Mihalache, G., Sellitto, V.M., Hlihor, R.-M., Stoleru, V., 2019. The Effects of a Microorganisms-Based Commercial Product on the Morphological, Biochemical and Yield of Tomato Plants under Two Different Water Regimes. Microorganisms 7, 706. https://doi.org/10.3390/microorganisms7120706

Jain, D., Shivani, Bhojiya, A.A., Singh, H., Daima, H.K., Singh, M., Mohanty, S.R., Stephen, B.J., Singh, A., 2020. Microbial Fabrication of Zinc Oxide Nanoparticles and Evaluation of Their Antimicrobial and Photocatalytic Properties. Front. Chem. 8. https://doi.org/10.3389/fchem.2020.00778

Jayarambabu, N., 2014. Germination and Growth Characteristics of Mungbean Seeds (Vigna radiata L.) affected by Synthesized Zinc Oxide Nanoparticles. International Journal of Current Engineering and Technology 4, 5.

Jiang, C., Zu, C., Lu, D., Zheng, Q., Shen, J., Wang, H., Li, D., 2017. Effect of exogenous selenium supply on photosynthesis, Na+ accumulation and antioxidative capacity of maize (Zea mays L.) under salinity stress. Sci. Rep 7, 42039.

Khan, S.T., Malik, A., Alwarthan, A., Shaik, M.R., 2022. The enormity of the zinc deficiency problem and available solutions; an overview. Arabian Journal of Chemistry 15, 103668. https://doi.org/10.1016/j.arabjc.2021.103668

Li, N., Wu, X., Zhuang, W., Xia, L., Chen, Y., Wu, C., Rao, Z., Du, L., Zhao, R., Yi, M., Wan, Q., Zhou, Y., 2021. Tomato and lycopene and multiple health outcomes: Umbrella review. Food Chemistry 343, 128396. https://doi.org/10.1016/j.foodchem.2020.128396

Li, Y., 2009. Physiological Responses of Tomato Seedlings (Lycopersicon Esculentum) to Salt Stress. Modern Applied Science 3, p171. https://doi.org/10.5539/mas.v3n3p171

Li, Yawen, Ye, Z., Xiang, J., Li, S., Zheng, Z., Li, Yichen, Fang, Y., Zhang, X., Chen, X., Xue, D., 2025. Purine nucleotide metabolism response to drought stress in rice. Plant Growth Regulation. https://doi.org/10.1007/s10725-025-01309-3

Maehly, A.C., 1954. The assay of catalases and peroxidases, in: Methods of Biochemical Analysis. Wiley, pp. 357–424. https://doi.org/10.1002/9780470110171.ch14

Mahalakshmi, H., Vijaya, 2020. In vitro biocompatibility and antimicrobial activities of zinc oxide nanoparticles (ZnO NPs) prepared by chemical and green synthetic route— A comparative study. BioNanoScience 10, 112–121. https://doi.org/10.1007/s12668-019-00698-w

Mahawar, L., Živčák, M., Barboricova, M., Kovár, M., Filaček, A., Ferencova, J., Vysoká, D.M., Brestič, M., 2024. Effect of copper oxide and zinc oxide nanoparticles on photosynthesis and physiology of *Raphanus sativus* L. under salinity stress. Plant Physiology and Biochemistry 206, 108281. https://doi.org/10.1016/j.plaphy.2023.108281

Manigopa, C., Sah, R., 2012. Genetic component in baby corn (Zea Mays L.) 12, 291–294.

Maurya, V.K., Kachhwaha, D., Bora, A., Khatri, P.K., Rathore, L., 2019. Determination of antifungal minimum inhibitory concentration and its clinical correlation among treatment failure cases of dermatophytosis. J Family Med Prim Care 8, 2577–2581. https://doi.org/10.4103/jfmpc.jfmpc_483_19

Medeiros, F.H.V., Martins, S.J., Zucchi, T.D., Melo, I.S., Batista, L.R., Machado, J.C., 2011. Biological control of mycotoxin-producing molds. Cienc. Agrotecnol 36, 483–497.

Meneguzzo, S., Navari-Izzo, F., Izzo, R., 1999. Antioxidative responses of shoots and roots of wheat to increasing NaCl concentrations. Journal of Plant Physiology 155, 274–280. https://doi.org/10.1016/S0176-1617(99)80019-4

Mishra, N., Jiang, C., Chen, L., Paul, A., Chatterjee, A., Shen, G., 2023. Achieving abiotic stress tolerance in plants through antioxidative defense mechanisms. Front. Plant Sci. 14. https://doi.org/10.3389/fpls.2023.1110622

Mittal, S., Kumari, N., Sharma, V., 2012. Differential response of salt stress on Brassica juncea: Photosynthetic performance, pigment, proline, D1 and antioxidant enzymes. Plant Physiol. Biochem 54, 17–26.

Mittova, V., Guy, M., Tal, M., Volokita, M., 2004. Salinity up-regulates the antioxidative system in root mitochondria and peroxisomes of the wild salt-tolerant tomato species Lycopersicon pennellii. Journal of Experimental Botany 55, 1105–1113. https://doi.org/10.1093/jxb/erh113

Modena, M.M., Rühle, B., Burg, T.P., Wuttke, S., 2019. Nanoparticle Characterization: What to Measure? Advanced Materials 31, 1901556. https://doi.org/10.1002/adma.201901556

Mogazy, A.M., Hanafy, R.S., 2022. Foliar Spray of Biosynthesized Zinc Oxide Nanoparticles Alleviate Salinity Stress Effect on Vicia faba Plants. J Soil Sci Plant Nutr 22, 2647–2662. https://doi.org/10.1007/s42729-022-00833-9

Munns, R., Tester, M., 2008. Mechanisms of salinity tolerance. Annu. Rev. Plant Biol 59, 651–681.

Murdock, R.C., Braydich-Stolle, L., Schrand, A.M., Schlager, J.J., Hussain, S.M., 2008. Characterization of nanomaterial dispersion in solution prior to in vitro exposure using dynamic light scattering technique. Toxicol Sci 101, 239–253. https://doi.org/10.1093/toxsci/kfm240

Nabati, J., Kafi, M., Nezami, A., Moghaddam, P.R., Ali, M., Mehrjerdi, M.Z., 2011. Effect of salinity on biomass production and activities of some key enzymatic antioxidants in Kochia (Kochia scoparia. Pak. J. Bot 43, 539–548.

Natasha, N., Shahid, M., Bibi, I., Iqbal, J., Khalid, S., Murtaza, B., Bakhat, H.F., Farooq, A.B.U., Amjad, M., Hammad, H.M., Niazi, N.K., Arshad, M., 2022. Zinc in soil-plant-human system: A data-analysis review. Science of The Total Environment 808, 152024. https://doi.org/10.1016/j.scitotenv.2021.152024

Nejati, K., Rezvani, Z., Pakizevand, R., 2011. Synthesis of ZnO nanoparticles and investigation of the ionic template effect on their size and shape. International Nano Letters 1, 75–81.
Noctor, G., Foyer, C.H., 1998. Ascorbate and Glutathione: Keeping Active Oxygen Under Control. Ann. Rev. Plant Physiol. Plant Mol. Biol 49, 249–279.
OmicsBox, 2019. Bioinformatics Made Easy. Valencia, BioBam Bioinformatics.
Pandit, M., Chakraborty, M., Haider, Z.A., Pande, A., Sah, R.P., Sourav, K., 2016. Genetic diversity assay of maize (Zea mays L.) inbreds based on morphometric traits and SSR markers. AJAR 11, 2118–2128. https://doi.org/10.5897/AJAR2015.10404
Parkhomchuk, D., Borodina, T., Amstislavskiy, V., Banaru, M., Hallen, L., Krobitsch, S., Lehrach, H., Soldatov, A., 2009. Transcriptome analysis by strand-specific sequencing of complementary DNA. Nucleic Acids Research 37, e123. https://doi.org/10.1093/nar/gkp596
Pitzschke, A., Forzani, C., Hirt, H., 2006. Reactive oxygen species signaling in plants. Antioxid. Redox Signal 8, 1757–1764.
Prud'homme, M.-P., Gonzalez, B., Billard, J.-P., Boucaud, J., 1992. Carbohydrate Content, Fructan and Sucrose Enzyme Activities in Roots, Stubble and Leaves of Ryegrass (*Lolium perenne* L.) as Affected by Source/Sink Modification after Cutting. Journal of Plant Physiology 140, 282–291. https://doi.org/10.1016/S0176-1617(11)81080-1
Quintero, J.M., Fournier, J.M., Benlloch, M., 2007. Na+ accumulation in shoot is related to water transport in K+-starved sunflower plants but not in plants with a normal K+ status. J. Plant Physiol 164, 60–67.
Rai-Kalal, P., Jajoo, A., 2021. Priming with zinc oxide nanoparticles improve germination and photosynthetic performance in wheat. Plant Physiology and Biochemistry 160, 341–351. https://doi.org/10.1016/j.plaphy.2021.01.032
Rasha, E., Monerah, A., Manal, A., Rehab, A., Mohammed, D., Doaa, E., 2021. Biosynthesis of Zinc Oxide Nanoparticles from Acacia nilotica (L.) Extract to Overcome Carbapenem-Resistant Klebsiella Pneumoniae. Molecules 26, 1919. https://doi.org/10.3390/molecules26071919
Sah, R., Ahmed, S., Malaviya, D., Saxena, P., 2016. Identification of consistence performing dual purpose maize (Zea mays L.) genotypes under semi-arid condition. Range Management and Agroforestry 37, 162–166.
Sah, R.P., Chakraborty, M., Prasad, K., Pandit, M., Tudu, V.K., Chakravarty, M.K., Narayan, S.C., Rana, M., Moharana, D., 2020. Impact of water deficit stress in maize: Phenology and yield components. Sci Rep 10, 2944. https://doi.org/10.1038/s41598-020-59689-7
Salih, A.M., Al-Qurainy, F., Khan, S., Tarroum, M., Nadeem, M., Shaikhaldein, H.O., Gaafar, A.-R.Z., Alfarraj, N.S., 2021. Biosynthesis of zinc oxide nanoparticles using Phoenix dactylifera and their effect on biomass and phytochemical compounds in Juniperus procera. Sci Rep 11, 19136. https://doi.org/10.1038/s41598-021-98607-3
Shaba.Zahra, Baghizadeh, A., Mohamadali, V., Yazdanpanah, A., Yousefi, M., 2010. The salicylic acid effect on the tomato (lycopersicum esculentum Mill) sugar, protein and proline contents under salinity stress (Nacl). Journal of Biophysics and Structural Biology.
Shalata, A., Neumann, P.M., 2001. Exogenous ascorbic acid (vitamin C) increases resistance to salt stress and reduces lipid peroxidation. Journal of Experimental Botany 52, 2207–2211. https://doi.org/10.1093/jexbot/52.364.2207
Shrivastava, P., Kumar, R., 2015. Soil salinity: A serious environmental issue and plant growth promoting bacteria as one of the tools for its alleviation. Saudi Journal of Biological Sciences 22, 123–131. https://doi.org/https://doi.org/10.1016/j.sjbs.2014.12.001
Smirnoff, N., 1998. Plant resistance to environmental stress. Current Opinion in Biotechnology 9, 214–219. https://doi.org/10.1016/S0958-1669(98)80118-3
Solaiman, M.A., Ali, M.A., Abdel-Moein, N.M., Mahmoud, E.A., 2020. Synthesis of Ag-NPs developed by green-chemically method and evaluation of antioxidant activities and anti-inflammatory of synthesized nanoparticles against LPS-induced NO in RAW 264.7 macrophages. Biocatalysis and Agricultural Biotechnology 29, 101832. https://doi.org/10.1016/j.bcab.2020.101832
Sun, L., Wang, Y., Wang, Ruling, Wang, Ruting, Zhang, P., Ju, Q., Xu, J., 2020. Physiological, transcriptomic, and metabolomic analyses reveal zinc oxide nanoparticles modulate plant growth in tomato. Environ. Sci.: Nano 7, 3587–3604. https://doi.org/10.1039/D0EN00723D
Tavallali, V., Rahemi, M., Eshghi, S., Kholdebarin, B., Ramezanian, A., 2010. Zinc alleviates salt stress and increases antioxidant enzyme activity in the leaves of pistachio (Pistacia vera L. 'Badami')

seedlings. Turkish Journal of Agriculture and Forestry 34, 349–359. https://doi.org/10.3906/tar-0905-10

Tavanti, T.R., Melo, A.A.R.D., Moreira, L.D.K., Sanchez, D.E.J., Silva, R.D.S., Silva, R.M.D., Reis, A.R.D., 2021. Micronutrient fertilization enhances ROS scavenging system for alleviation of abiotic stresses in plants. Plant Physiology and Biochemistry 160, 386–396. https://doi.org/10.1016/j.plaphy.2021.01.040

Tsubouchi, H., Yamamoto, K., Hisada, K., Sakabe, Y., Udagawa, S., 1987. Effect of roasting on ochratoxin A level in green coffee beans inoculated with Aspergillus ochraceus. Mycopathologia 97, 111–115.

Tunc-Ozdemir, M., Miller, G., Song, L., Kim, J., A, S., 2009. Thiamin confers enhanced tolerance to oxidative stress in arabidopsis. Plant Physiol 151, 421–432.

Venisse, J.-S., Gullner, G., Brisset, M.-N., 2001. Evidence for the Involvement of an Oxidative Stress in the Initiation of Infection of Pear by Erwinia amylovora 1. Plant Physiology 125, 2164–2172. https://doi.org/10.1104/pp.125.4.2164

Vokkaliga T, H., Wu, T.-M., Hong, C.-Y., 2017. Glutathione Reductase and Abiotic Stress Tolerance in Plants, in: Glutathione in Plant Growth, Development, and Stress Tolerance. pp. 265–286. https://doi.org/10.1007/978-3-319-66682-2_12

Wiegand, I., Hilpert, K., Hancock, R.E.W., 2008. Agar and broth dilution methods to determine the minimal inhibitory concentration (MIC) of antimicrobial substances. Nat Protoc 3, 163–175. https://doi.org/10.1038/nprot.2007.521

Yedurkar, S., Maurya, C., Mahanwar, P., 2016. Biosynthesis of Zinc Oxide Nanoparticles Using Ixora Coccinea Leaf Extract—A Green Approach. Open Journal of Synthesis Theory and Applications 5, 1–14. https://doi.org/10.4236/ojsta.2016.51001

Yin, Y.-G., Kobayashi, Y., Sanuki, A., Kondo, S., Fukuda, N., Ezura, H., Sugaya, S., Matsukura, C., 2010. Salinity induces carbohydrate accumulation and sugar-regulated starch biosynthetic genes in tomato (Solanum lycopersicum L. cv. 'Micro-Tom') fruits in an ABA- and osmotic stress-independent manner. J Exp Bot 61, 563–574. https://doi.org/10.1093/jxb/erp333

Yusof, Z.N.B., 2019. Thiamine and Its Role in Protection Against Stress in Plants (Enhancement in Thiamine Content for Nutritional Quality Improvement), in: Jaiwal, P.K., Chhillar, A.K., Chaudhary, D., Jaiwal, R. (Eds.), Nutritional Quality Improvement in Plants. Springer International Publishing, Cham, pp. 177–186. https://doi.org/10.1007/978-3-319-95354-0_7

Zafar, S., Hasnain, Z., Aslam, N., Mumtaz, S., Jaafar, H.Z., Wahab, P.E.M., Qayum, M., Ormenisan, A.N., 2021. Impact of Zn Nanoparticles Synthesized via Green and Chemical Approach on Okra (Abelmoschus esculentus L.) Growth under Salt Stress. Sustainability 13, 3694. https://doi.org/10.3390/su13073694

Zafar, S., Perveen, S., Kamran Khan, M., Shaheen, M.R., Hussain, R., Sarwar, N., Rashid, S., Nafees, M., Farid, G., Alamri, S., Shah, A.A., Javed, T., Irfan, M., Siddiqui, M.H., 2022. Effect of zinc nanoparticles seed priming and foliar application on the growth and physio-biochemical indices of spinach (Spinacia oleracea L.) under salt stress. PLoS One 17, e0263194. https://doi.org/10.1371/journal.pone.0263194

Zak, A.K., Abrishami, M.E., Majid, W.H.Abd., Yousefi, R., Hosseini, S.M., 2011a. Effects of annealing temperature on some structural and optical properties of ZnO nanoparticles prepared by a modified sol–gel combustion method. Ceramics International 37, 393–398. https://doi.org/10.1016/j.ceramint.2010.08.017

Zak, A.K., Majid, W.H.Abd., Darroudi, M., Yousefi, R., 2011b. Synthesis and characterization of ZnO nanoparticles prepared in gelatin media. Materials Letters 65, 70–73. https://doi.org/10.1016/j.matlet.2010.09.029

Zak, A.K., Razali, R., Majid, W.A., Darroudi, M., 2011c. Synthesis and characterization of a narrow size distribution of zinc oxide nanoparticles. IJN 6, 1399–1403. https://doi.org/10.2147/IJN.S19693